PHILOSOPHICAL TRANSACTIONS OF THE ROYAL SOCIETY A MATHEMATICAL, PHYSICAL & ENGINEERING SCIENCES

The Lake Mungo Geomagnetic Excursion

M. F. Barbetti and M. W. McElhinny

Phil. Trans. R. Soc. Lond. A 1976 **281**, 515-542
doi: 10.1098/rsta.1976.0048

THE LAKE MUNGO GEOMAGNETIC EXCURSION

By M. F. Barbetti† and M. W. McElhinny
Research School of Earth Sciences, Australian National University, Canberra, A.C.T., Australia

(*Communicated by S. K. Runcorn, F.R.S. – Received 16 September 1975*)

CONTENTS

Archaeomagnetic studies have been made of prehistoric aboriginal fireplaces occurring along the ancient shore of Lake Mungo, a dried out lake in southeastern Australia. Directions of magnetization preserved in ovenstones and baked hearths show that wide departures of up to 120° from the axial dipole field direction occurred about 30000 years ago. The determination of the variation in geomagnetic field strength from the baked material is complicated by non-ideal behaviour during Thellier's double heating method. The problem appears to arise from the subsequent (post-firing) formation of iron oxyhydroxides during a period in which the water level in the lake rose. During laboratory heatings these oxyhydroxides dehydrate causing the non-ideal behaviour observed. The ancient field strengths deduced are therefore probably minimum values. The geomagnetic excursion recorded between at least 30780 ± 520 and 28140 ± 370 years b.p. on the conventional radiocarbon time scale is associated with very high field strengths between 1 and 2 Oe (1 Oe $\approx$ 79.6 A m^{-1}). The field strength subsequently decreased to between 0.2 and 0.3 Oe after the excursion. This main excursion is referred to as the Lake Mungo geomagnetic excursion. There is evidence that a second excursion associated with low field strengths of 0.1–0.2 Oe occurred around 26000 years b.p.

† Present address: Research Laboratory for Archaeology, 6 Keble Road, Oxford, OX1 3QJ.

A review of geomagnetic excursions less than 40 000 years in age shows that it may be premature to assume that these are world-wide synchronous features. The range of ages and their groupings in different parts of the world may indicate they are temporary non-dipole features of continental extent. However, the duration of most excursions (order of 10^3 years) is very similar to that of polarity transitions and this could indicate they are aborted reversals.

1. Introduction

That the Earth's magnetic field has reversed itself frequently in the past is now a well-established fact; the history of polarity changes over the last four to five million years has been summarized by Cox (1969). During polarity changes it is observed that the geomagnetic field direction swings through about 180°, and that the virtual geomagnetic poles (v.g.p.) for different transitions follow widely diverse paths. This could be interpreted as the result of a decrease in the main dipole field, so that the observed field is dominated by the non-dipole field. However, Dagley & Lawley (1974) have pointed out that there are also certain similarities, and particularly sharp east–west changes in the longitude of transitional v.g.p., which suggest that the field is controlled by a dipole with independently varying axial and equatorial components. On the basis of the available data, Dagley & Lawley concluded that neither model by itself is clearly preferred, but that a combination of dipole and non-dipole sources might explain the observations.

The time estimated for the geomagnetic field to undergo a polarity transition is of the order of 10^3–10^4 years (Cox & Dalrymple 1967; Ninkovich, Opdyke, Heezen & Foster 1966; McElhinny 1971). It is observed that the virtual dipole moment (v.d.m.) decreases during a transition to about one-quarter of the values observed when the geomagnetic field has a nearly-axial configuration, and that it increases again as the opposite polarity is established; there is some evidence of transitory increases in strength just before some polarity changes when the v.g.p. is about 40° from the geographic north pole (Wilson, Dagley & McCormack 1972; Dagley & Lawley 1974). Evidence has also been presented for a transitory increase in field strength during the central part of a polarity transition when the v.g.p. is near the equator (Shaw 1975).

In addition to polarity changes it has been observed that the Earth's magnetic field has often departed from its usual near-axial configuration for brief periods, without establishing and perhaps not even instantaneously approaching a reversed direction. This type of behaviour is now usually termed a *geomagnetic excursion* (Denham & Cox 1971; Doell & Cox 1972; Barbetti & McElhinny 1972) and has previously been referred to by some authors as sudden departures or systematic deviations (Lawley 1970). Geomagnetic excursions have also been reported from lava flows of various ages in different parts of the world (Doell 1972; Doell & Cox 1972; Doell & Dalrymple 1973; Ellwood, Watkins, Amerigian & Self 1973; Lawley 1970; Watkins & Nougier 1973; Watkins 1973), and from some deep-sea and lake sediments (Clark & Kennett 1973; Denham & Cox 1971; Nakajima *et al.* 1973; Opdyke, Shackleton & Hays 1974; Freed & Healy 1974). We have previously reported the occurrence of a geomagnetic excursion observed in Australian aboriginal fireplaces from Lake Mungo (Barbetti & McElhinny, 1972). Excursions are generally observed to start with a sudden and often fairly smooth movement of the v.g.p. towards equatorial latitudes. The v.g.p. may then return almost immediately, or it may cross the equator and move through latitudes in the opposite hemisphere before swinging back again to resume a near-axial position. In this paper, we use the term excursion to describe v.g.p. movement

more than 40° *from the geographic pole* (following the suggestion of Wilson, Dagley & McCormack (1972) for intermediate pole positions) *which terminates with a return of the Earth's field to its pre-existing polarity, without the dynamo being observed to establish itself in the opposite polarity*. Defined in this way excursions are differentiated from the secular variation (when the v.g.p. colatitude θ exceeds 40°) and from short polarity events – a term we apply only when the opposite polarity ($\theta \leqslant 40°$ or $\theta \geqslant 140°$) persists long enough for at least one oscillation in the strength of the main dipole field (about 10^4 years).

There is already some evidence that geomagnetic excursions may take less time than polarity transitions; for example, Denham & Cox (1971) estimate 600 years for the excursion recorded in sediments at Mono Lake in California. At Lake Mungo the departures from the dipole field direction appear to cover about 2500 years (Barbetti & McElhinny 1972). Freed & Healy (1974) estimate 2500 years for the duration of an excursion with the same age recorded in the Gulf of Mexico. Lawley (1970) has shown that the field strength decreased during some excursions (termed 'systematic deviations' by Lawley) recorded in lava flows in eastern Iceland and several other authors have reported a low intensity of magnetization, suggesting that a reduced field strength is a common feature of geomagnetic excursions.

In this paper we report a detailed investigation of the Lake Mungo geomagnetic excursion. An unusual feature is the evidence for a large increase in field strength during part of this excursion, which may provide new information on processes occurring in the Earth's core.

2. Locality and sampling

2.1. *Lake Mungo*

Inland southeastern Australia, west of the Great Dividing Range and foothills, is an area of low relief less than 200 m above sea level. A major river system, comprising the Murray, Darling, Murrumbidgee, Lachlan and other tributary rivers, carries run-off water from the ranges westwards through this flat semi-arid region, and eventually to the sea in South Australia (see inset figure 1). The area contains numerous ancient lakes – particularly where the continental dunefield has, in the past, extended into and interfered with the western part of the Murray–Darling drainage system.

Lake Mungo is one of a chain of dried lakes which forms the terminal system of the Willandra Creek, a distributary stream which leaves the Lachlan River some 250 km to the east and now carries water only when major flooding of the Lachlan occurs. At various times during the Pleistocene, however, the flow was sufficient to maintain a high water level in the lakes for long periods.

The Quaternary geology of the Willandra lakes has been described in detail by Bowler (1971 *a*, *b*) and in Bowler, Jones, Allen & Thorne (1970). In plan, the lakes have cliffed western margins and long high transverse dunes (lunettes) around their eastern shores. Three soil-stratigraphic units are recognized in the lunettes (figure 1). The basal Golgol unit consists of a deep, red calcareous soil developed on quartz sands, and is beyond the range of radiocarbon dating. The lakes were re-activated some time before about 40 000 b.p. and subsequent high water levels resulted in the deposition of the quartz sands of the overlying Mungo unit. At about 25 000 years b.p. the lakes became almost dry, and in many places calcareous and argillaceous silty sands were deposited in the lunettes. The top of the thin Mungo unit is marked by soil development. Part of the overlying Zanci unit consists of quartz sands deflated from high level

PHILOSOPHICAL TRANSACTIONS OF THE ROYAL SOCIETY A MATHEMATICAL, PHYSICAL & ENGINEERING SCIENCES

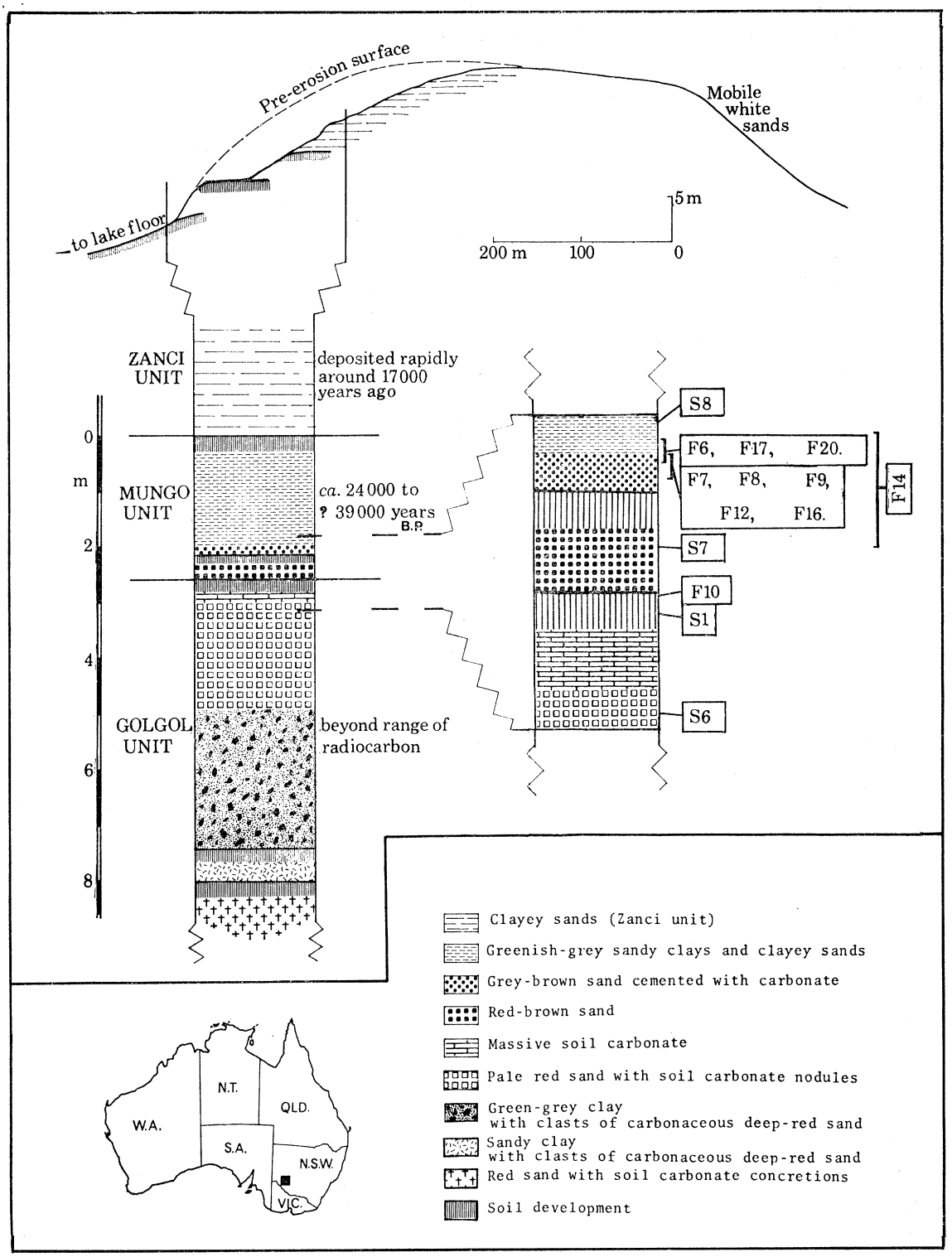

FIGURE 1. Lunette stratigraphy with positions of the fireplaces and sediment samples. Lake Mungo is located by the square on the inset map. A transverse section through the lunette is shown at the top, and details of the stratigraphy as exposed by modern erosion are given in the stratigraphic column on the left. The soil sedimentary units and their ages are those given by Bowler (1971*a*, *b*). On the right, part of the column is expanded to show the relative stratigraphic position of the fireplaces and sediment samples.

PHILOSOPHICAL TRANSACTIONS OF THE ROYAL SOCIETY A MATHEMATICAL, PHYSICAL & ENGINEERING SCIENCES

beaches after about 23 500 years b.p., although most of the unit (up to 32 m thick) was deposited rapidly during progressive drying of the lakes between 17 500 years and 16 000 years b.p. These lakes have remained inactive since about 15 000 years b.p.

Prehistoric man exploited the varied resources in and around the Willandra lakes when they were active during the late Pleistocene (Allen 1972). The earliest evidence for human occupation yet detected in this area comes from the high water shoreline deposits of the Mungo unit, and a number of sites around Lake Mungo contain relics dating between 24 000 years and 32 000 years b.p.; these have been summarized by Barbetti & Allen (1972). The present investigation concerns some ancient fireplaces preserved in these sediments and exposed by modern erosion, located between 5 and 6 km from the southernmost end of the Mungo lunette. There are also some fireplaces in the younger Zanci unit, and numerous fireplaces on the lake floors, shorelines and surrounding plains with ages ranging from modern to *ca.* 5000 years b.p. Some of these fireplaces have also been investigated (Barbetti & Polach 1973; Barbetti 1973*a*), and although details of the archaeomagnetic measurements have yet to be published we mention some general conclusions in this paper.

2.2. *Aboriginal fireplaces*

Three types of ancient fireplaces are found in the region. Aboriginal *ovens* consist of cooking stones (or substitute lumps of earth or clay) arranged on top of a thin band of ash and charcoal in a shallow depression. Small areas of blackened earth without cooking stones, resulting from an open fire, are termed *hearths*. We have also investigated two well-preserved *mounds of baked clay*, which might have been a different type of oven, or, alternatively, were fireplaces with some unknown purpose.

Figure 1 shows a generalized stratigraphic column and the positions of the ten fireplaces and four (unbaked) sediment horizons sampled at Lake Mungo during this investigation. Even over the restricted area of these sites (about 700 m long) there is considerable variation in the thickness, colour and lithology of the sedimentary layers, reflecting the variability of dune-building processes. For example at the site of a group of fireplaces (F6, F7, F8, F9, F12; figure 2) the top 50 cm or more of the Golgol unit was locally eroded prior to deposition of the overlying Mungo unit, and the zone of weak soil development near the base of the Mungo unit is also absent. This, together with the fact that detailed Golgol stratigraphy is not usually exposed by modern erosion on the lunette, made it difficult to identify the top of the Golgol unit, and it was at first incorrectly assigned to the soil horizon near the base of the stratigraphic column (Barbetti & Allen 1972). The re-assessment presented here was made only after further field investigation and discussion with J. M. Bowler.

Clay-sand oven stones which had not been disturbed by modern erosion were oriented by using both Sun and magnetic compasses, and in some cases groups of small ovenstones were sampled as a block in the same way as the baked sediment underneath the fireplaces. Samples of the porous and friable sediment were obtained by carving around and isolating a stump of material, without moving it; this was then coated with commercially available polyurethane foam, with an aluminium plate set in the top for orienting the sample before removal. Polyurethane foam, rather than plaster as is commonly used for archaeomagnetic sampling (see, for example, Aitken 1970), was selected because it sets quickly (20 min), has a low density, does not wet the sample, and forms a 'crushable' (rather than rigid) protective coating suitable for transportation. A disadvantage of foam is the slight warping which may occur during the first few weeks after setting; this necessitates placing the aluminium plate (for orienting) in the

centre of the coating, with only a thin film of polyurethane between it and the top of the baked earth sample. Charcoal samples for radiocarbon dating were collected separately during excavation.

Five of the fireplaces (F6, F7, F8, F9 and F12) were found close together and details of the positions of baked sediment samples, together with unbaked sediment samples S6, S7 and S8, are shown in figure 2. Oven F14, 30 m north from this group, was badly eroded at the time of discovery; several displaced ovenstones and one oriented sample of baked sediment from the base were collected. 'Fireplace' F10 consisted of a few small fragments of baked clay-sand embedded in the top few centimetres of the Golgol unit, and is not necessarily of human origin;

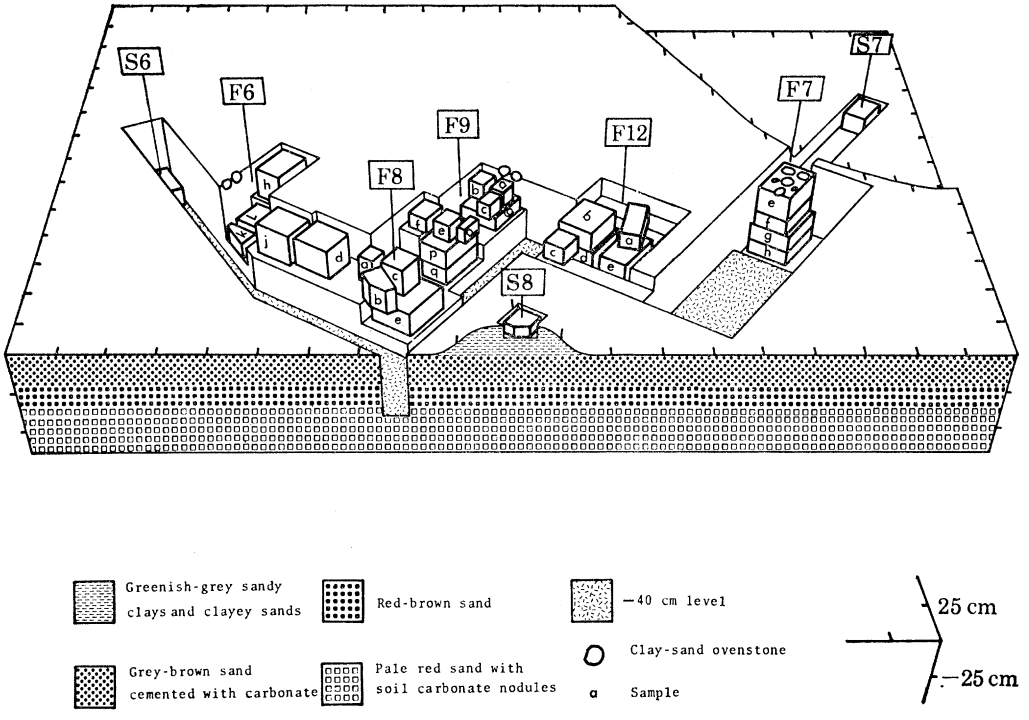

FIGURE 2. Perspective diagram showing the provenance of samples from the main group of fireplaces and the surrounding unbaked sediment. Block samples are identified by letters. The front of the diagram is approximately north–south, with north to the right.

no charcoal was found and one oriented sample, including the baked fragments and underlying sediment, was taken. Sediment sample S1 was taken from the top of the Golgol soil near F10, about 100 m north of F14. About 250 m further north, a mound of very friable baked clay (F16) was found and three oriented samples were taken; from the baked clay (sample A), the underlying 10 cm thick ash layer (B) and the sediment beneath it (C); a further piece of baked clay, partly detached from the mound, was collected with the flat uppermost surface identified (sample L). Unoriented baked clay-sand ovenstones and charcoal were collected from a nearby oven (F17) which had been bodily moved downhill by erosion. The tenth fireplace (oven F20) was located about 350 m *south* of the main group of five fireplaces, within the sandy clay of the Mungo unit; one oriented sample with two clay-sand ovenstones was obtained, but the underlying sediment which had swelled and become plastic after heavy rain was not sampled. Locality details are given in Barbetti (1973*a*).

At the laboratory, as many cores (28 mm diameter) as possible were cut from the samples, using a converted drilling machine with a phosphor-bronze coring tube, and compressed air to remove the cuttings. Great care was necessary, and in many cases the coring tube was turned slowly by hand. In the case of sediment samples, it was necessary to harden the extracted cores with commercially-available waterglass solution, before slicing the cores into 28 mm long cylindrical specimens. Clay-sand ovenstones specimens were not hardened. Commercial waterglass is made by dissolving sodium metasilicate (Na_2SiO_3) in water, under pressure. The solution is considerably hydrolysed by the reaction:

$$Na_2SiO_3 + 2H_2O \rightleftharpoons 2Na^+ + 2OH^- + H_2SiO_3.$$

When the sediment is dipped in waterglass, a slow reaction (over one or two days) occurs with the natural pedogenic calcium carbonate to form insoluble calcium silicate, which makes a much stronger heat-resistant cement between the sand silt grains. We looked for, but did not observe, any effects of this process on the specimen magnetization.

TABLE 1. ^{14}C AGES FOR LAKE MUNGO FIREPLACES

fireplace	type	^{14}C sample no.	number of analyses	^{14}C age years b.p. (5568 year half-life)
F6	oven	ANU-667	1	26270 ± 470
F7	oven	ANU-680	3	30780 ± 520
F8	hearth	ANU-681	2	28310 ± 410
F9	oven	ANU-682	3	27530 ± 340
F12	hearth	ANU-683	2	28000 ± 410
F16	mound	ANU-685	2	28140 ± 370
F17	oven	ANU-686	1	25570 ± 520
F20	oven	ANU-698†	1	25310 ± 810

† Unpublished datum (obtained on alkali-insoluble charcoal fraction).

Conventional ages (calculated using the 5568 year half life) are given with their *standard* errors. Column 4 gives the number of samples collected and analysed separately. Details of methods and individual results are given by Barbetti & Polach (1973) and Barbetti (1973*a*).

3. AGE

At the time of discovery, the stratigraphic positions of the fireplaces within the Mungo unit indicated that all their ages were greater than 24000 years b.p., based on the radiocarbon chronology previously established by Bowler (1971*a*, *b*). On field evidence, we thought that fireplaces F6, F17, F20 would be slightly younger than F7, F8, F9, F12 and F16, because of their position at the base of the clayey silts above the grey-brown sand horizon (figure 1). No charcoal was available from oven F14 for dating, and even details of the stratigraphic position could not be determined accurately, so that its age can only be roughly estimated to be between 25000 and *ca.* 35000 b.p. Fireplace F10 also lacked charcoal, but its stratigraphic position on top of the Golgol soil indicates a minimal age of 35000 years b.p. Unbaked sediment samples S6 and S1 have been affected by the long period of Golgol soil formation which ended before *ca.* 40000 years b.p.; actual deposition may well have taken place prior to 50000 or 60000 years b.p. Sample S7 was deposited at some time between *ca.* 40000 and 32000 years b.p. (but was stratigraphically younger than S1 and F10), and sample S8 was deposited at 24500 ± 500 years b.p.

The radiocarbon ages obtained on charcoal from the fireplaces (table 1) are entirely consistent with the stratigraphic evidence. Wherever possible, two or even three samples were collected

from the area of each fireplace and dated separately to test for possible mixing of charcoal from contiguous fireplaces; and in two cases (F7, F16) measurements on charcoal collected from underneath baked material (which later archaeomagnetic measurements showed had not been disturbed since cooling) were compared with results from charcoal collected nearby, but sealed only by sediment. We found no evidence for mixed sources of charcoal, and duplicate analyses were combined to give conventional ^{14}C ages with a high precision. The accuracy of these ages in terms of absolute years B.P. depends on the ancient concentration of atmospheric radiocarbon, and this has not yet been established (Barbetti 1972, 1973*a*).

An attempt was made to determine the relative ages of contiguous fireplaces with indistinguishable ^{14}C ages by thermal demagnetization experiments on oriented specimens of baked sediment collected from overlapping parts of the fireplaces. It was hoped that such material might preserve two directions of magnetization in different parts of the blocking temperature spectrum, with the magnetization acquired through partial reheating by the younger fireplace residing in the lower temperature part of the spectrum, superimposed on the magnetization relating to the older fireplace. However, we did not find material with two distinct partial magnetizations, and this experiment was therefore not successful.

We have also submitted samples for thermoluminescent dating to the Research Laboratory for Archaeology at Oxford, and the ages estimated by this independent method are broadly consistent with our radiocarbon ages (M. J. Aitken & J. Huxtable, private communication).

4. Archaeomagnetic measurements

4.1. *Directions of magnetization*

A routine procedure was adopted for study of the natural remanent magnetization (n.r.m.). Some measurements of specimen direction and intensity of magnetization were made with an astatic magnetometer (described by Manwaring 1971), but most measurements were made with a Schonstedt SSM-1 5 Hz spinner magnetometer. Thermal demagnetization was carried out in a furnace designed by Barbetti (1973*b*) in an automatically controlled field-free space described by McElhinny, Luck & Edwards (1971). The initial n.r.m. and its direction after thermal cleaning at 100 °C was measured for each specimen. Some selected specimens, mostly from suspected zones of disturbance, were further demagnetized in increasing steps of 100 °C, but most specimens were reserved for possible ancient field strength measurements which, when carried out, included demagnetization in steps of less than 100 °C. In all cases, there was no significant change in direction during thermal cleaning above 100 °C until the intensity of magnetization had been reduced to a small fraction of its original value ($\lesssim 0.25$ for unbaked sediment; $\lesssim 0.1$ for baked material).

Mean directions of magnetization for all fireplaces and sediment samples are listed in table 2. Most fireplaces gave very consistent results, and *specimen* directions of magnetization after thermal cleaning are illustrated in figure 3. For oven F7 (figure 3*a*) specimens from ovenstone samples B and D show internally consistent directions, but the sample means differ from those of the other samples indicating that they had been slightly displaced since cooling; they were omitted in calculating the site mean (table 2). Specimen directions for F8 are more dispersed than those of F7, and this probably reflects differences in the amount of settling and compaction occurring after baking of the sediment. We found that specimens from samples D, E, F, P and Q of oven F9 gave consistent directions, although specimens from samples

TABLE 2. DIRECTIONS OF MAGNETIZATION AFTER THERMAL CLEANING AT 100 °C

fireplace or sediment	sample	material	n	sample mean D/deg	sample mean I/deg	site mean D_m/deg	site mean I_m/deg	k	α_{95}	position of virtual North Pole
S1	A	u	2	4.9	−64.5	—	—	167	19.5	308° E, 77° N
S6	A	u	5	295.2	−35.6	—	—	249	4.9	49° E, 31° N
S7	A	b?	4	272.8	−10.4	—	—	567	3.9	50° E, 5° N
S8	A	u	3	359.7	−52.3	—	—	121	11.2	126° E, 89° N
F6	H	b	7	116.1	−7.1	—	—	227	4.0	—
F6	J	b	3	88.9	−7.3	90.4	−10.7	526	5.4	238° E, 3° N
	K	b	9	91.6	−13.8	($N = 3$, $R = 2.9962$)				
	L	b	15	90.8	−10.9					
F7	B	o	4	251.1	+20.3	—	—	381	4.7	—
	D	o	6	255.1	+8.2	—	—	796	2.4	—
F7	A	o	2	232.0	+8.3	236.6	+1.7	251	4.2	34° E, 28° S
	C	o	4	237.0	+1.6	($N = 6$, $R = 5.9801$)				
	E	b	12	238.3	+2.4					
	F	b	8	237.5	+0.2					
	G	b	6	232.7	−0.1					
	H	b	9	241.6	−2.2					
F8	A	b	2	84.4	−11.0	78.0	−9.7	115	7.2	230° E, 13° N
	B	b	9	70.6	−17.5	($N = 5$, $R = 4.9653$)				
	C	b	11	78.8	−8.2					
	D	b	7	82.4	−7.4					
	E	b	12	73.6	−4.4					
F9	A	b	5	132.8	+1.3	—	—	490	3.5	—
	B	b	8	119.1	+3.8	—	—	491	2.5	—
	C	b	1	106.8	−1.6	—	—	—	—	—
	G	b	6	109.9	+10.0	—	—	22	14.5	—
	D	b	3	100.4	+2.4	99.3	+0.3	362	4.0	238° E, 8° S
	E	b	4	95.2	−1.4	($N = 5$, $R = 4.9889$)				
	F	b	2	102.8	−2.7					
	P	b	13	95.7	+1.5					
	Q	b	10	102.5	+1.5					
F10	A†	u	10	19.6	−66.6	—	—	167	3.7	—
F12	B	b	9	224.6	+0.2	—	—	33	9.1	—
	D	b	17	199.9	−11.0	—	—	2.6	28.1	—
F12	A	b	12	257.4	−6.1	262.0	−3.2	80	13.9	47° E, 6° S
	C	b	4	256.8	+0.3	($N = 3$, $R = 2.9750$)				
	E	b	20	271.8	−3.8					
F14	A	b	11	190.0	−13.8	—	—	14	12.6	—
F16	A†	c	1	31.9	−75.5	—	—	—	—	Ca n.g.p.‡
	B	b	5	349.2	−63.5	—	—	25	15.5	
	L	c	7	—	Ca-45	—	—	—	—	
F16	C	u	18	353.6	−70.0	—	—	106	3.4	
F17	no oriented samples									Ca n.g.p.
F20	A	o	2	15.4	−59.3	—	—	186	18.4	Ca n.g.p.

† Direction without thermal cleaning. ‡ n.g.p., north *geographic* pole.

b, baked sediment; c, baked clay; o, baked clay–sand ovenstone and u, unbaked sediment; identification based on magnetic characteristics and archaeological evidence.

n is the number of specimens measured, N the number of samples and R the resultant of N unit vectors.

D, I are the declination (east of true north) and inclination (positive downwards) for each sample and D_m, I_m the corresponding values for site means.

k is the Fisher (1953) precision parameter and α_{95} the radius of the circle of 95% confidence about either sample or site mean direction.

Examples are illustrated in figure 3.

A, B, C and G (from another part of the oven, see figure 2) gave very scattered directions (figure 3*b*). A large scatter in specimen directions of magnetization (up to 100°; figure 3*b*) was also observed in the adjacent samples B and D of hearth F12, and an examination of the exact positioning of the specimens indicated that the variation is the result of some superimposed (possibly human?) disturbance. Data from these disturbed areas were not used in calculating means for fireplaces F9 and F12 (table 2). There is also some scatter in specimen directions of magnetization for oven F14 (figure 3*c*) indicating possible post-baking disturbance; these

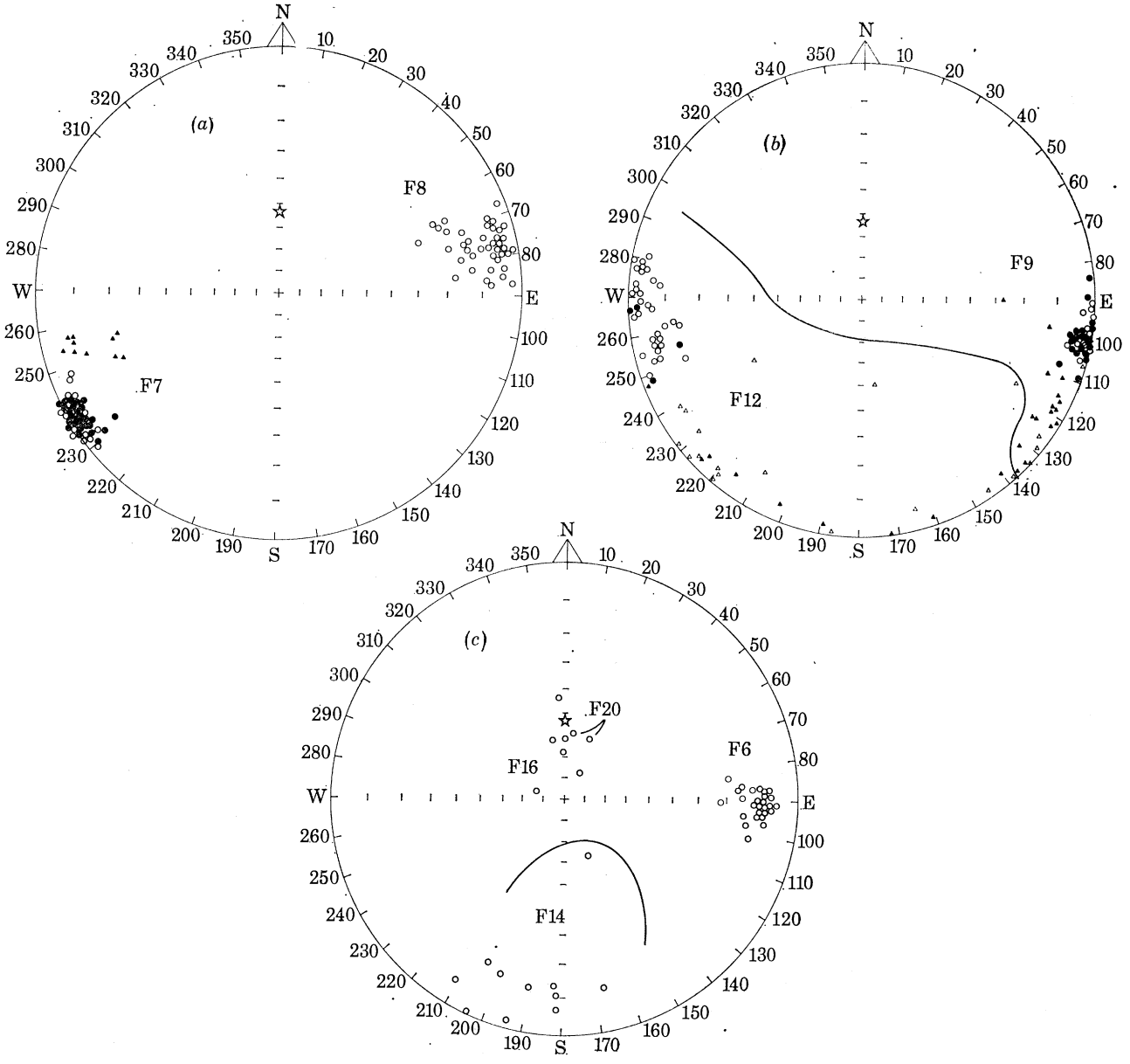

FIGURE 3. Stereographic projections of specimen directions of magnetization after thermal cleaning at 100 °C. Open (solid) symbols indicate negative (positive) inclination, with the circles (triangles) denoting measurements used (excluded) in the calculation of the fireplace mean directions (table 2). The star indicates the axial dipole field direction (0°, −53°) at the locality.

specimens are all from the one oriented sample. Figure 3*c* also illustrates directions from F16 (specimens from samples A and B), F20 and F6 (specimens from samples J, K and L). For oven F6, the direction of magnetization of sample H differs significantly from that of samples K and L and has not been included in the mean (table 2); it is possible that this sample (located alongside the oven; figure 2) may have been magnetized by a separate (undated) fire.

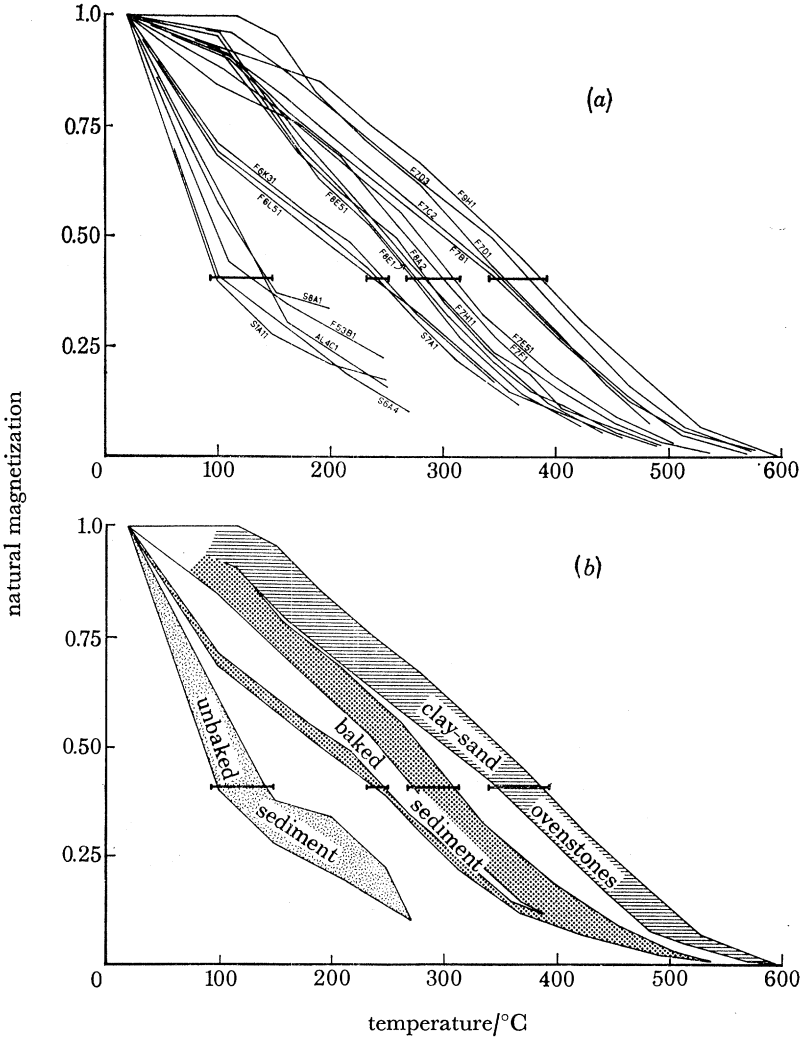

FIGURE 4. (*a*) Thermal demagnetization curves for typical specimens of unbaked sediment, baked sediment from fireplaces F6, F7, F8 and the undisturbed parts of F9, and ovenstones from F7 and F9. Moments are normalized with total n.r.m. taken as unity. The curves fall into three main groups, as illustrated in (*b*). Some ovenstone specimens from F6, F14, F17 and F20, as well as the baked clay specimens from F16, have demagnetization curves which are convex upwards and lie above and to the right of those shown. Apart from these exceptions all the measured thermal demagnetization curves fall within the group boundaries outlined in (*b*).

4.2. *Thermal demagnetization curves*

The different types of material have characteristic thermal demagnetization curves as illustrated in figure 4. For specimens of ovenstone and baked sediment, the magnetization is concentrated in the middle and upper parts of the blocking temperature spectrum and is directionally stable to more than 350 °C. On the other hand, the magnetization in three specimens of unbaked sediment is not stable above 250 °C, and more than half of it resides in grains

with blocking temperatures below 150 °C. There is also a difference of about one order of magnitude in the intensity of total n.r.m. for baked and unbaked materials. These results reflect the different origins of the magnetization; thermoremanent for the baked material, viscous and/or chemical (but not detrital) for the unbaked sediment. We used these characteristics to infer that sample F10-A and sample F16-C comprise material which had not been baked above *ca.* 200 °C, and that the magnetization of sample S7 may possibly be thermoremanent in origin (column 3, table 2).

Samples from all the fireplaces (except F10) have a stable thermoremanent magnetization, and record some wide departures of the geomagnetic field from the axial dipole direction. The interpretation of these results is discussed later in the paper. We note here that the magnetization of the unbaked sediments, deposited under aeolian conditions some tens of thousands of years ago in a semi-arid environment, is still in the process of stabilization. This suggests that the *chemical remanent magnetization* (c.r.m.) observed in terrestrial sediments only dates from a late stage of compaction and consolidation. In the present instance, it appears that the magnetization of the unbaked sediments cannot be related stratigraphically to that of the fireplaces.

5. Ancient field strengths

5.1. *Thellier's method*

Measurements of the ancient geomagnetic field strengths were made by using the Thellier method (Thellier & Thellier 1959), following the procedure described in detail by Coe (1967*a*). In the laboratory the n.r.m. is gradually removed by controlled heating and cooling cycles, repeated twice for each temperature, at successively higher temperatures. After the first heating the specimen is cooled in zero magnetic field, and the remaining natural magnetization is measured. The specimen is then reheated to exactly the same temperature and cooled in a measured weak magnetic field to give it an artificial *partial thermoremanent magnetization* (p.t.r.m.) in addition to the remaining n.r.m. If the distribution of t.r.m. with temperature (the t.r.m. spectrum) remains unchanged and Thellier's (1951) law of additivity of p.t.r.m. is obeyed, then the ratio of the partial n.r.m. and artificial p.t.r.m. will be the same in each temperature interval. When t.r.m. is linear with field, this ratio is equal to the ratio of the ancient geomagnetic and laboratory field strengths. The double heating method ensures that the p.t.r.m. is acquired at each temperature before the specimen has been heated to higher temperatures, thus avoiding as much as possible the effects of mineralogical or phase changes which might occur at high temperatures.

The results of the paired heatings on a specimen can conveniently be presented as a diagram, with the remaining partial n.r.m. plotted (as the ordinate) against the acquired artificial p.t.r.m. at each temperature step (an *n.r.m.–t.r.m. diagram*). For an ideal specimen, the points would lie on a straight line with negative slope equal to the ratio of the ancient geomagnetic and laboratory field strengths (Nagata, Arai & Momose 1963; Coe 1967*a*). In practice, experimental errors result in a small scatter of the points, and the method of least squares can be used to obtain the best estimate b of the true slope β. A confidence interval may be placed on β, using the student t distribution.

We adopted a standard procedure, in which ten specimens were selected and processed together. Heatings were accomplished in a specially designed non-inductive electrical furnace containing ten specimens placed 5 cm apart, using a heating time of exactly 60 min (with the

preselected temperature being reached after approximately 40 min, and held for about 20 min) and a cooling time of about 40 min (Barbetti 1973*b*). Specimens were replaced in the same positions for successive heating cycles, and the temperatures for repeat heatings did not differ by more than 1 °C. The double heatings were continued with temperature steps between 30 °C and 100 °C until a significant directional change in n.r.m. was observed; in practice this did not occur until the specimens had been almost completely demagnetized. P.t.r.m. *tests*, in which cooling from some intermediate temperature in the laboratory field is repeated after double heatings have been made at higher temperatures, were made on selected specimens.

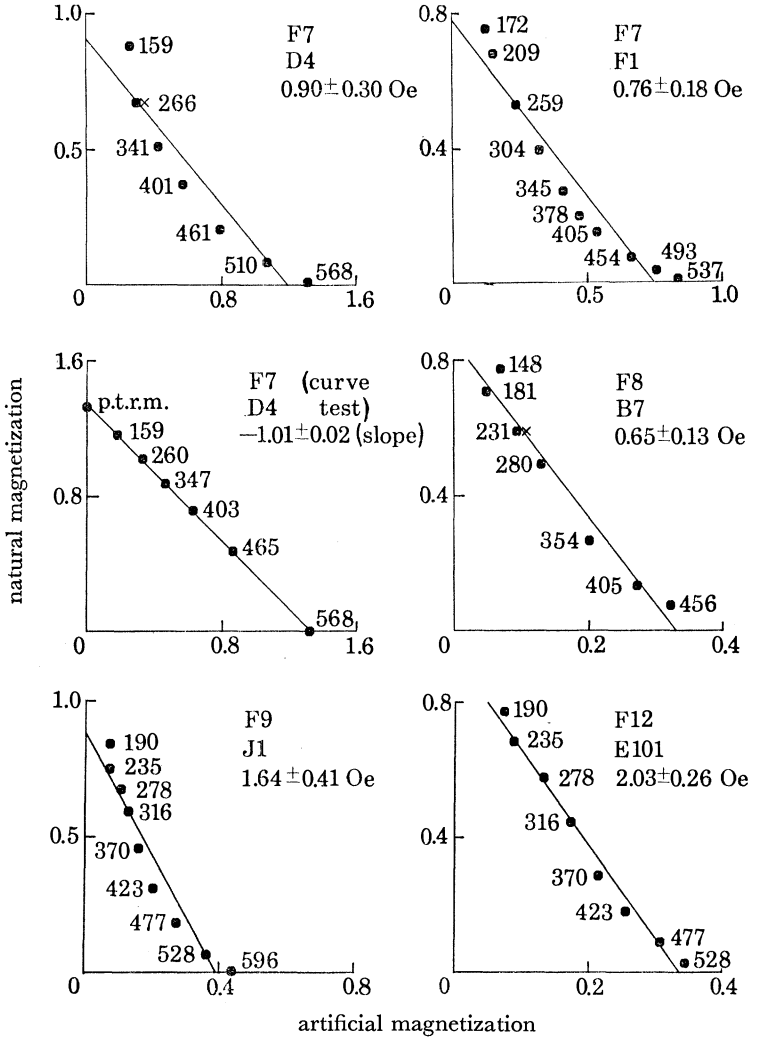

FIGURE 5. Typical n.r.m.–t.r.m. diagrams for fireplaces F7, F8, F9 and F12. Moments are normalized, with total n.r.m. taken as unity. Numbers near the circles indicate the heating temperature (unit: °C), with results from p.t.r.m. tests represented by a cross. Least-squares fitted lines are shown, and the corresponding estimates of ancient field strength are given with formal 95% confidence limits.

Figures 5 and 6 illustrate some representative n.r.m.–t.r.m. diagrams. Least squares straight lines were calculated with unit weight assigned to all points except the total n.r.m., which was excluded because of the possibility of a viscous component of magnetization, and the corresponding values of ancient field strength are quoted with 95% confidence limits. We did not

Table 3. Summary of ancient geomagnetic induction measurements

fireplace or sediment	specimen	material	total n.r.m. (10^{-5} emu g^{-1})	laboratory field/Oe	ancient field strength/Oe	mean/Oe	I_m/deg	α_{95}/deg	virtual dipole moment 10^{25} G cm^3
S7	A1	b?	7.3	0.25	0.17 ± 0.05	—	—	—	—
F6	H5	b	11	0.73	0.22 ± 0.09	—	—	—	—
F6	A1	o	17	0.25	0.18 ± 0.02	0.15 ± 0.03	-10.7	5.4	3.8 ± 0.8
	B1	o	11	0.59	0.14 ± 0.01				
	B2	o	12	0.25	0.12 ± 0.01				
	C1	o	25	0.25	0.17 ± 0.01				
	C2	o	28	0.25	0.20 ± 0.02				
	K31	b	4.1	0.25	0.09 ± 0.03				
F7	A1	o	99	0.25	1.52 ± 0.37	1.09 ± 0.18	$+1.7$	4.2	28.1 ± 4.6
	B1	o	161	1.19	1.32 ± 0.25				
	C2	o	53	1.19	0.85 ± 0.24				
	D1	o	88	0.25	1.14 ± 0.25				
	D2	o	76	0.73	1.03 ± 0.30				
	D3	o	68	1.19	0.97 ± 0.34				
	D4	o	73	1.19	0.90 ± 0.30				
F7	E11	b	26	0.59	0.69 ± 0.24	0.73 ± 0.03	$+1.7$	4.2	18.8 ± 0.8
	E51	b	26	1.19	0.65 ± 0.17				
	F1	b	33	0.73	0.76 ± 0.18				
	F2	b	32	0.73	0.77 ± 0.17				
	F3	b	37	0.59	0.76 ± 0.29				
	F5	b	28	1.19	0.78 ± 0.23				
	G1	b	25	0.73	0.68 ± 0.15				
	G7	b	22	0.73	0.79 ± 0.14				
	H11	b	17	0.73	0.74 ± 0.15				
	H3	b	18	0.73	0.71 ± 0.15				
F8	A2	b	29	0.25	0.55 ± 0.12	0.59 ± 0.07	-9.7	7.2	15.1 ± 1.8
	B41	b	33	0.25	0.73 ± 0.14				
	B5	b	22	0.25	0.53 ± 0.15				
	B7	b	26	0.25	0.65 ± 0.13				
	B71	b	34	0.25	0.64 ± 0.12				
	E1	b	23	0.73	0.47 ± 0.12				
	E51	b	28	0.73	0.57 ± 0.14				
F9	J1	o	135	0.73	1.64 ± 0.41	1.56 ± 0.16	$+0.3$	4.0	40.2 ± 4.1
	H1	o	131	0.73	1.48 ± 0.38				
F9	D1	b	57	0.59	1.12 ± 0.40	0.85 ± 0.21	$+0.3$	4.0	21.9 ± 5.4
	E3	b	41	0.59	0.87 ± 0.26				
	P1	b	38	0.73	0.81 ± 0.16				
	Q3	b	34	0.73	0.61 ± 0.12				
F12	E100	b	71	0.73	1.62 ± 0.25	1.83 ± 0.42	-3.2	13.9	47.2 ± 10.9
	E101	b	85	0.73	2.03 ± 0.26				
F12	B2	b	24	0.59	0.47 ± 0.07	—	—	—	—
F14	A21	b	5.2	0.25	0.14 ± 0.05	0.13 ± 0.02	-13.8	12.6	3.4 ± 0.4
	A7	b	5.6	0.73	0.13 ± 0.03				
	G1	o	12	0.25	0.12 ± 0.02				
	H1	o	12	0.25	0.15 ± 0.03				
	X1	o	11	0.25	0.10 ± 0.01				
	Y1	o	16	0.25	0.15 ± 0.01				
F16	L2	c	32	0.25	0.37 ± 0.02	0.31 ± 0.07	-53	20	5.8 ± 1.9
	L31	c	53	0.25	0.22 ± 0.06				
	L4	c	92	0.25	0.36 ± 0.11				
	L5	c	36	0.25	0.29 ± 0.03				
F17	A1	o	29	0.25	0.23 ± 0.02	0.21 ± 0.03	-53	20	4.0 ± 1.0
	B1	o	29	0.25	0.19 ± 0.02				
	C1	o	24	0.25	0.23 ± 0.02				
F20	A1	o	32	0.25	0.28 ± 0.02	0.28 ± 0.01	-53	20	5.3 ± 1.2
	A2	o	29	0.25	0.28 ± 0.01				
	B1	o	27	0.25	0.28 ± 0.02				

b, baked sediment; c, baked clay and o, baked clay–sand ovenstone.

Values of ancient field strength and virtual dipole moment are listed with formal 95% confidence limits.

I_m (the site mean inclination) and α_{95} (the 95% confidence limit for I_m) are taken from table 2, with values of $-53°$ (the axial dipol inclination) and 20°, respectively, assumed for fireplaces F16, F17 and F20.

PHILOSOPHICAL TRANSACTIONS OF THE ROYAL SOCIETY A MATHEMATICAL, PHYSICAL & ENGINEERING SCIENCES

exclude any other data, even though many of the n.r.m.–t.r.m. diagrams showed a marked curvature; for these specimens, the wide confidence limits of the estimated field strength essentially reflect the degree of curvature. The small contribution of measurement errors (using the Schonstedt magnetometer) is illustrated by an experiment in which a laboratory p.t.r.m. of specimen F7D4 was treated as an n.r.m. and a 'field strength' measurement made in the same laboratory field. The points of the n.r.m.–t.r.m. diagram (F7D4 – curve test; figure 5) define a straight line with slope very close to the expected value of -1. A few ancient field strength measurements were made by using an astatic magnetometer (described by Manwaring 1971) which we found to be slightly less accurate than the spinner magnetometer (note the comparatively large scatter of points for F8B7, figure 5). P.t.r.m. tests tended to give slightly greater repeat values (as illustrated for F7D4 and F8B7; figure 5), but the individual differences are within experimental error. This observation and possible reasons for curvature in the n.r.m.–t.r.m. diagram are discussed in the next section, in which we show that including all points in the calculation is likely to give a *low* value for the slope. If this is correct then values of the ancient field strength can probably be regarded as minimum estimates.

5.2. *Results*

All the ancient field strengths determined are summarized in table 3. Sample S7, as noted in the previous section, was found to have a more stable magnetization than other sediment samples; a field strength measurement on specimen A1 gave an acceptable n.r.m.–t.r.m. diagram and a low value for the ancient field strength. Measurements on a specimen from F6 sample H (which has a direction of magnetization significantly different from other samples of F6) also gave a low value for the ancient field strength, which precludes any possibility of its magnetization being contemporary with F9. A specimen from sample B of F12 gave a value significantly lower than specimens from sample E, which is consistent with the directional evidence that sample B comprises material which was disturbed after baking.

For F6, F14, F17 and F20 there is very little curvature in the n.r.m.–t.r.m. diagrams (see figure 6) and good agreement between specimens from the same fireplace, irrespective of the type of material in the case of F6 and F14 (table 3). Specimens from these five fireplaces give values for the ancient field strength considerably less than the present-day field strength at the site. In contrast with this, specimens from fireplaces F7, F8, F9 and F12 give much higher values for the ancient field strength and often exhibit considerable curvature in their n.r.m.–t.r.m. diagrams (see figure 5). In the case of F7 and F9 there appears to be some difference between results from ovenstone and baked sediment, with the former giving slightly higher values. This presumably reflects some minor variation in the processes which caused the observed non-ideal behaviour.

In table 3 mean values of the ancient field strength are given with formal 95% confidence limits, which reflects the variation *between* specimens rather than the uncertainty due to curvature in the n.r.m.–t.r.m. diagrams. Corresponding values of the virtual dipole moment (v.d.m.) were calculated (after Smith 1967) using the expression

$$M = \tfrac{1}{2} H_{\mathrm{m}} r^3 (1 + 3\cos^2 I_{\mathrm{m}})^{+\frac{1}{2}},$$

where H_{m} is the mean ancient geomagnetic field strength, r the radius of the Earth, and I_{m} the site mean inclination.

The confidence limits on M only take account of the uncertainties in I_{m} as well as H_{m}, and therefore do not reflect the uncertainty arising from the curvature in the n.r.m.–t.r.m. diagrams.

We believe values for M derived from material with little curvature in the n.r.m.–t.r.m. diagrams to be essentially correct, whereas values derived from material with substantial curvature are probably *less* than the true values. The evidence for this assertion is discussed in the next section.

6. Non-ideal behaviour with Thellier's method

6.1. *General considerations*

Following the measurements of ancient field strength using Thellier's method on six specimens from F7, Thellier's method was repeated on the *artificial* magnetization acquired during cooling from about 560 °C in a field of 1.19 Oe. The resulting 't.r.m.–t.r.m.' diagrams showed no curvature and gave well defined lines with slopes equal, within experimental error, to the expected slope of -1 (for example, F7D4 curve test in figure 5). This indicated that the laboratory p.t.r.m. were reproducible with good precision *after the first series of heatings* and therefore that the equipment being used was not at fault in any way. Other experiments were then carried out to try and determine the cause of the curvature of the n.r.m.–t.r.m. diagrams.

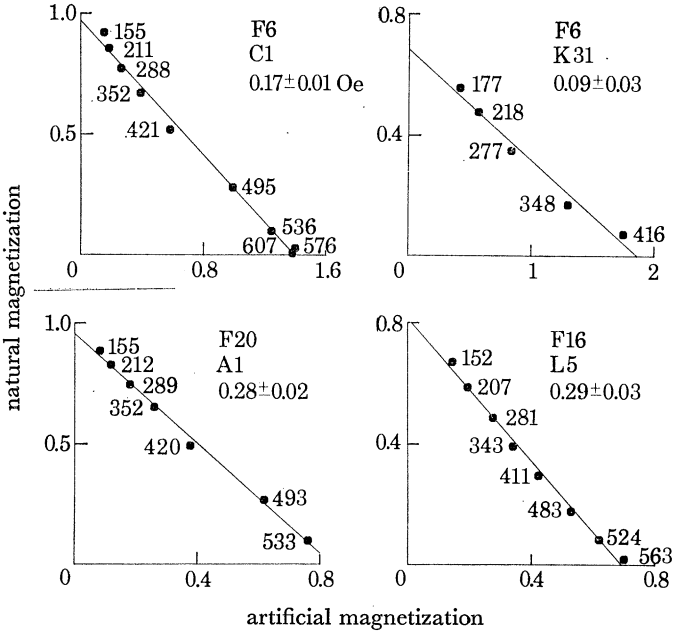

Figure 6. Typical n.r.m.–t.r.m. diagrams for fireplaces F6, F16 and F20. Notation is the same as in figure 5.

Coe (1967*b*) has described several possible mechanisms which might be responsible for systematic curvature in n.t.m.–t.r.m. diagrams. In an archaeological context there are other possibilities and these together may be summarized as follows

(1) the presence of multidomain grains,

(2) disparities in the original and laboratory cooling rates,

(3) changes in the demagnetizing field associated with the cutting of specimens for laboratory experiments,

(4) non-linearity of t.r.m. with applied field,

(5) superimposition of secondary *isothermal* components of magnetization on the original n.r.m. at or since the time of cooling,

(6) superimposition of other *thermal* components of magnetization on the original n.r.m. at or since the time of cooling,

(7) irreversible changes in the t.r.m. spectrum during laboratory experiments due to mineralogical, chemical or phase changes.

Of these mechanisms (1) and (2) are unlikely to be significant in archaeomagnetic investigations when the material consists of fine-grained haematite dispersed in a clay–sand matrix. A high field Curie temperature was obtained for an ovenstone from F6 and gave a value of 620 °C with no sign of any magnetite Curie temperature during the heating and cooling. The effect of change in demagnetizing factor associated with the cutting of the specimens (3) was eliminated as a possible cause of curvature by allowing the artificial magnetization to be directed anti-parallel to the n.r.m. during the stepwise heatings for three specimens. The n.r.m.–t.r.m. diagrams did not show the opposite (i.e. convex-upwards) curvature to be expected (Coe 1967*b*) if the change in demagnetizing factor was significant (for example F9J1 and F12E101, figure 5).

When the ancient and laboratory field strengths differ, a curvature in the n.r.m.–t.r.m. diagram may result if the p.t.r.m. is non-linear with field (4) in some parts of the blocking temperature spectrum and linear in other parts (Coe 1967*b*). This possibility seemed unlikely because of the similar shape of the n.r.m.–t.r.m. curves regardless of applied field in the laboratory. However a direct test was performed on ten virgin specimens by measuring the p.t.r.m. acquired by cooling from 330 °C and also from 530 °C in five successively higher fields up to 1.25 Oe. No departure from linearity of p.t.r.m. with applied field was detected.

6.2. *Secondary isothermal components*

It is possible that secondary isothermal components of magnetization have been superimposed on the original n.r.m. since the time of cooling (5). During thermal demagnetization there is generally a small change in direction of a few degrees up to 100 °C and thereafter the directions remain constant at higher temperatures. This indicates the presence of a small v.r.m. component which is easily demagnetized. Is it possible, however, that the bulk of the magnetization is made up of i.r.m. such as might be observed from a lightning strike? To test this possibility we have compared the alternating field demagnetization curves of n.r.m. and t.r.m. of specimens from the same fireplace. These curves have very similar shapes (figure 7). Although there is a rapid decrease in intensity of n.r.m. at low alternating fields, a common characteristic of specimens with large i.r.m. components, this feature is also a property of the t.r.m. The concentration of the magnetization of the specimens in the low coercivity part of the spectrum is therefore a property of the magnetic material, probably related to the grain size distribution (a preponderance of small grains only just larger than the superparamagnetic size). As a further check the alternating field demagnetization characteristics of the n.r.m. of one specimen were compared with those of an a.r.m. acquired using a peak alternating field of 1500 Oe with steady field bias of 1.34 Oe. The coercivity spectrum of n.r.m. and a.r.m. is virtually identical for alternating fields above 50 Oe (inset of figure 7). Below 50 Oe a small viscous component is being removed from the n.r.m. The ratio a.r.m./n.r.m., assuming the ancient field value for F6 given in table 3 and that its n.r.m. is a t.r.m., is then of the order

PHILOSOPHICAL TRANSACTIONS OF THE ROYAL SOCIETY A MATHEMATICAL, PHYSICAL & ENGINEERING SCIENCES

of 0.1. Low values such as this are typical a.r.m./t.r.m. values expected from samples containing only single domain grains (Levi 1974).

The data of figure 7 do not necessarily exclude the possibility that the n.r.m. is all of chemical origin because t.r.m. and c.r.m. have very similar demagnetization properties (Kobayashi 1959). However it has already been shown in §4 that the blocking temperature spectrum of unbaked sediment extends up to no higher 250–300 °C (figure 4). The observation that the directions of magnetization of the fireplaces are stable up to at least 600 °C therefore excludes the possibility that grains with blocking temperatures above 300 °C have ordinary c.r.m. The evidence thus strongly favours the view that the n.r.m. of these fireplaces is a t.r.m. with a minor v.r.m. component that is readily demagnetized at low temperatures (100 °C) and low alternating fields (50 Oe).

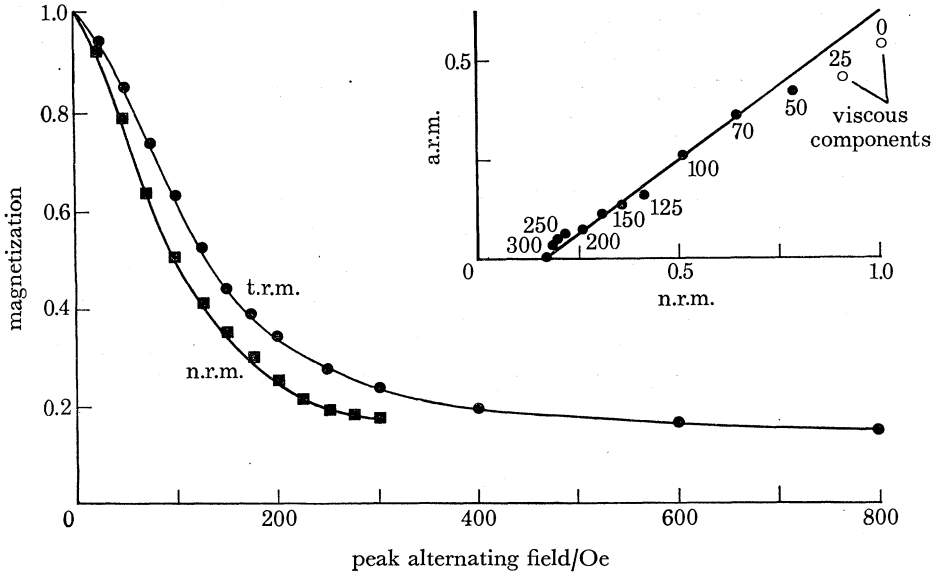

FIGURE 7. Normalized alternating field demagnetization curves for two specimens from F6. One specimen had a laboratory t.r.m., acquired by cooling from 680 °C in a field of 0.59 Oe. The n.r.m. of another specimen was demagnetized in steps to 300 Oe (lower curve) and then given an a.r.m. using a peak alternating field of 1500 Oe and tumbling the specimen in a holder with a steady field of 1.34 Oe. When progressively demagnetized the a.r.m. showed a linear relation with n.r.m. for alternating fields above 50 Oe (inset; numbers near points give the alternating field in Oe; magnetization values normalized to total n.r.m.). N.r.m. and a.r.m. measurements by courtesy of J. Shaw, Liverpool University.

6.3. *Thermochemical effects and later heatings*

Although we have provided evidence that the magnetization of the fireplaces is essentially t.r.m. in origin, can we be certain that the t.r.m. spectrum is not composed of components with different origins? It is possible that the fireplaces were originally heated to only (say) 400 °C, and that some chemical reaction and/or grain growth occurred which enabled magnetization to be blocked in grains which we now observe to have blocking temperatures much higher than 400 °C. Schwarz & Christie (1967) have suggested that a similar process occurred in some potsherds from Ontario. We shall refer to such magnetization in blocking temperatures above the firing temperature as thermo-chemical remanent magnetization (t.c.r.m.). The experiments of Porath (1968) however suggest that the ability of specimens to acquire c.r.m. is only about one-tenth of their ability to acquire t.r.m. in the same field. Therefore if the higher

blocking temperatures have been derived from t.c.r.m. the resulting n.r.m.–t.r.m. diagram would be expected to show a marked decrease in slope (by a factor of about ten) above the temperature of initial firing (see figure 8*a*). Furthermore, there should be no change in direction associated with the t.c.r.m. Interpretation of some of our n.r.m.–t.r.m. diagrams in terms of such a two stage model is possible because changes in slope of up to a factor of 4 or 5 can be deduced. However, the correct value of ancient field strength would then be derived from the *initial* slope of the n.r.m.–t.r.m. diagram. In that case the field strength derived from a least squares fit of all the data points (as in table 3) would give a *minimum* value.

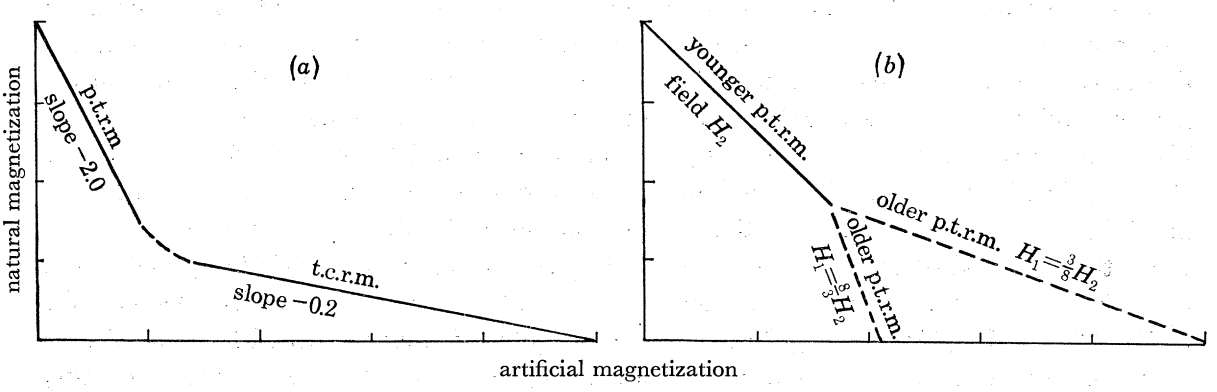

FIGURE 8. Hypothetical n.r.m.–t.r.m. diagrams. (*a*) For material which was originally baked once at a temperature below the Curie point and (in addition to an ordinary p.t.r.m. acquired during rapid cooling) has a magnetization residing in grains with higher blocking temperatures, acquired by a process involving grain formation or grain growth during baking (a thermochemical remanent magnetization, or t.c.r.m.). Assuming there are no other factors causing non-ideal behaviour, a Thellier measurement (in this case with laboratory field strength of 0.5 times the ancient field strength) would yield two straight line segments. The initial part of the diagram, relating to the p.t.r.m., would have the correct slope of -2. Above the temperature of the original baking the line would have a slope of -0.2, assuming the efficiency of t.c.r.m. acquisition to be uniformly about one-tenth that of p.t.r.m. acquisition. Note that there would be no change in the *direction* of magnetization associated with the change in slope (provided the material had not been moved during heating or cooling). (*b*) For material which has been baked on two separate occasions, firstly in a field with strength H_1 and subsequently in a field H_2, with a significantly lower temperature being achieved during the second (younger) heating. Using a laboratory field of strength H_2, a Thellier measurement would yield a straight line of slope -1 until the maximum temperature of the younger original baking was reached. At higher temperatures, a straight line segment with different slope would be observed if the ancient field strengths H_1 and H_2 differed. Two examples are illustrated; in one case $H_1 = \frac{3}{8}H_2$, and in the other $H_1 = \frac{8}{3}H_2$. If the two ancient field *directions* differed significantly, or if the material was moved after the first baking, a continuous change in specimen direction of magnetization would be observed while the younger p.t.r.m. was being erased.

A change of slope in the n.r.m.–t.r.m. diagram would also be observed if the fireplaces had been subjected to a second heating to some temperature below the original firing temperature. This possibility can be excluded for the fireplaces recording the excursion because it would be expected that the younger p.t.r.m. would have a different direction of magnetization compared with the older p.t.r.m. and this is not observed. For the fireplaces recording the normal dipole field direction a change of slope would occur without significant directional change if the field strengths in which the older and younger p.t.r.m.s were acquired were markedly different (figure 8*b*). However, on this hypothesis the concave–downward n.r.m.–t.r.m. diagrams would only be observed if the younger p.t.r.m. was always acquired in a field greater than the older p.t.r.m. In the reverse situation convex–upward n.r.m.–t.r.m. diagrams would be observed (figure 8*b*). It would be somewhat coincidental if the relative field strengths were always in the

PHILOSOPHICAL TRANSACTIONS OF THE ROYAL SOCIETY A MATHEMATICAL, PHYSICAL & ENGINEERING SCIENCES

correct sense to produce concave–down n.r.m.–t.r.m. diagrams as we observe. In any case the field strength corresponding to the last heating is given by the *initial* slope of the n.r.m.–t.r.m. diagram. Again this would mean that our estimates of field strength in table 3 are *minimum* values.

6.4. *Chemical changes produced in the laboratory*

Finally we consider the possibility that irreversible changes in the t.r.m. spectrum during laboratory experiments due to mineralogical, chemical or phase changes (7) have occurred. It seems improbable that the ovenstones, situated close to the hottest part of the fire, would not have been heated close to or above the Curie temperature of haematite. Therefore the dehydration of any hydrated minerals present would have been completed during the original firing, and the prolonged heating would certainly have produced a very stable mineral assemblage. If the curvature in the n.r.m.–t.r.m. diagrams is to be explained by mineralogical or chemical changes, then it must result from some mineral formed *after* the initial firing. The most likely possibility appears to be the formation of iron oxyhydroxides during a period in which the water table was raised above the level of the fireplaces subsequent to their firing and burial beneath younger sediments. The obvious candidates are the iron oxyhydroxides goethite (α-FeOOH) and lepidocrocite (γ-FeOOH). These hydrated minerals would have acquired a c.r.m. on formation but this would have made negligible contribution to the n.r.m. intensity because the process produces an exceedingly weak c.r.m. (Hedley 1968). Upon heating specimens during Thellier experiments the iron oxyhydroxides would have dehydrated to haematite. Goethite reverts to haematite at about 300 °C and lepidocrocite reverts initially to maghaemite at about 300 °C and then to haematite at about 450 °C (Hedley 1968; Strangway, Honea, McMahon & Larson 1968; Strangway, McMahon & Bischoff 1969; Vlasov & Gornushkina 1973).

An examination of thin sections indeed shows the presence of various hydrated minerals. Silica grains (silt size) were coated with calcite, various clay minerals and a fine red mineral presumed to be haematite. Originally the colour of ovenstone specimens ranged from yellow to orange (presumed to be limonite) or a grey-black colour arising from organic matter which had not fully oxidized in the original firing. The baked sediments ranged from red-brown to pale red. Upon heating the organic matter gradually disappears and a slight reddening in colour was observed at temperatures above 500 °C. The observed colour changes are consistent with the dehydration of lepidocrocite to haematite (Vlasov & Gornushkina 1973).

In figure 9 we model possible ways in which the dehydration of goethite or lepidocrocite to haematite might cause curvature in the n.r.m.–t.r.m. diagrams. The original c.r.m. of these minerals contributes virtually nothing to the total n.r.m. Large amounts of goethite have to be invoked so that on dehydration to haematite (assumed to take place completely at 300 °C) a change in slope of the n.r.m.–t.r.m. diagram is produced due to the increased capability of acquiring p.t.r.m. 25–50% of the final haematite needs to have been derived from goethite to produce any pronounced curvature such as we observe (figure 9*a*). The effects are much more pronounced with lepidocrocite (figure 9*b*). The assumed initial reversion to maghaemite produces a sharp change in slope (between 225 and 300 °C) with only 0.5% lepidocrocite because maghaemite is capable of acquiring 130 times the p.t.r.m. as the same quantity of haematite. Upon reversion to haematite around 450 °C the p.t.r.m. capability is reduced again and another change of slope occurs. In practice of course the changes are not as abrupt as we

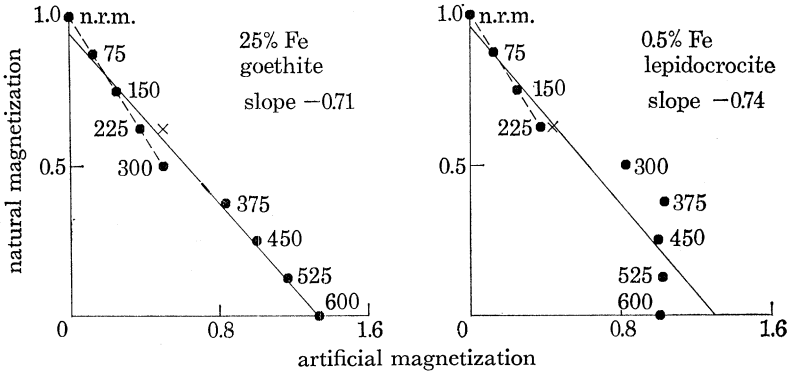

FIGURE 9. Hypothetical n.r.m.–t.r.m. diagrams for specimens which contained only haematite at the time of original cooling from 600 °C, and in which the resulting t.r.m. was distributed evenly over the blocking temperature spectrum from 0 to 600 °C. Subsequently, a fraction of the haematite was converted into one of the iron oxyhydroxides without loss or gain of iron in the specimens and, for simplicity, without the oxyhydroxides acquiring a remanent magnetization. A Thellier measurement is then made, using a laboratory magnetic field with the same strength as the original field. In (*a*) 25% of the haematite grains have been completely altered to form goethite grains which remain passive until reverting to haematite grains (again evenly distributed in blocking temperatures) between 300 and 375 °C. In (*b*) 0.5% of the haematite grains have been completely altered to form lepidocrocite grains, which dehydrate to form maghaemite grains between 225 and 300 °C. The maghaemite grains are assumed to be randomly oriented and evenly distributed over the blocking temperature spectrum. Those grains with appropriate blocking temperatures then acquire a t.r.m. (130 times stronger than for haematite) as they cool in the laboratory field. Above 375 °C the maghaemite begins to revert to haematite, and this process is assumed to be half completed at 450 °C, three-quarters completed at 525 °C and completed at 600 °C. In both (*a*) and (*b*) the cross shows the result of a hypothetical p.t.r.m. test performed at 225 °C after laboratory heating to 600 °C. We note that the correct slope of −1 (dashed line) would be obtained from the *low* temperature part of each n.r.m.–t.r.m. diagram *before* chemical changes begin to occur in the laboratory heating. A least-squares analysis of all the points (solid line) would give a lower slope and hence a low estimate of ancient field strength. Actual processes are likely to be considerably more complicated than the simple model described, but in a general way we can say that the weathering of t.r.m.-bearing haematite will lead to a *low* estimate of ancient field strength if the specimen recovers its full t.r.m.-bearing capacity during laboratory heating.

TABLE 4. PARTIAL THERMOREMANENT MAGNETIZATION TESTS

specimen	p.t.r.m. at	test after	p.t.r.m. first value	p.t.r.m. repeat value	artificial field/Oe
F6 B1	248 °C	500 °C	1.096	1.145	0.59
F6 C2	217	329	0.199	0.200	0.25
F7 A1	235	359	0.033	0.039	0.25
F7 B1	269	512	0.353	0.349	1.19
F7 C2	268	514	0.356	0.366	1.19
F7 D1	231	344	0.034	0.055	0.25
F7 D3	268	514	0.236	0.310	1.19
F7 D4	266	510	0.296	0.346	1.19
F7 E51	263	503	0.529	0.526	1.19
F7 F5	260	497	0.451	0.460	1.19

Comparison of first measurement of p.t.r.m. at given temperature with second p.t.r.m. acquired at same temperature, after stepwise heating has progressed to higher temperature. P.t.r.m. moments are normalized, with initial total n.r.m. of each specimen taken as unity.

PHILOSOPHICAL TRANSACTIONS OF THE ROYAL SOCIETY A MATHEMATICAL, PHYSICAL & ENGINEERING SCIENCES

have modelled in figure 9, but it appears that the presence of very small quantities of lepidocrocite could be the cause of the curvature in the n.r.m.–t.r.m. diagrams.

Repeat determinations of p.t.r.m. (p.t.r.m. tests) were made on several specimens during the Thellier heatings. After heating to much higher temperatures, the p.t.r.m. cooling from about 250 °C was repeated (table 4). Agreement is within experimental error. Some of these repeat determinations are indicated by a cross on the n.r.m.–t.r.m. diagrams of figure 5. The calculated position of such a p.t.r.m. test at 250 °C is also indicated by a cross on figure 9. The repeat determination is expected to lie close to the original at this temperature. During some of the Thellier heatings susceptibility was monitored at various temperatures as shown in table 5. There is a small decrease in susceptibility with temperature, as has been observed previously to accompany the dehydration of iron oxyhydroxides (Collinson 1968).

TABLE 5. SPECIFIC SUSCEPTIBILITY MEASUREMENTS

	susceptibility/(10^{-7} G cm^3 g^{-1} Oe^{-1}) after heating to				
specimen	initial	130 °C	330 °C	370 °C	530 °C
F6 B99†	127	128	128	124	126
F7 B11†	138	136	130	122	125
F7 F6‡	27.3	25.7	26.2	24.7	20.6
F7 F97	34.0	—	—	—	30.5
F7 F98	32.0	—	—	—	29.1
F7 F99	31.8	—	—	—	29.1
F7 G89‡	27.4	25.7	23.5	22.7	19.6
F7 H99‡	18.8	18.2	18.2	18.0	15.6
F8 C1‡	44.0	42.9	43.6	40.6	36.4
F8 E97‡	33.6	30.5	30.7	30.2	25.4
F9 E2‡	43.6	42.3	42.2	39.2	34.9
F9 Q97‡	37.7	35.2	34.2	34.3	27.1
F14 G1†	—	96	89	88	95
F14 H1†	—	66	64	64	64
F17 B99†	133	129	128	126	126

† Ovenstone specimen. ‡ Treated with waterglass hardening solution.

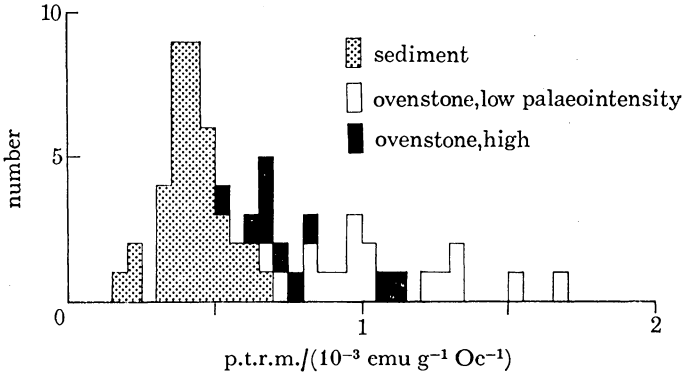

FIGURE 10. Histogram of specific thermoremanence acquired during laboratory cooling from about 560 °C for 66 specimens. Specimens of baked sediment have a narrow range as might be expected for a limited thickness of sediment. Ovenstone specimens have a much wider range, the higher values reflecting a generally higher content of haematite grains with appropriate blocking temperatures. This indicates a variation in the nature of the original material. Estimates of ancient field strength were consistent for each fireplace regardless of the type of material.

We attempted to detect changes in J_s–T curves to show the possible formation of maghaemite during heating, but our apparatus was not sensitive enough to detect the changes that would arise from such small amounts of lepidocrocite. If either of the dehydration processes is the cause of the curvature in the n.r.m.–t.r.m. diagrams then once again it is the *initial* slope of the diagram that provides the correct ancient field strength. The values shown in table 3 from a least squares fit to all the points represent *minimum* values.

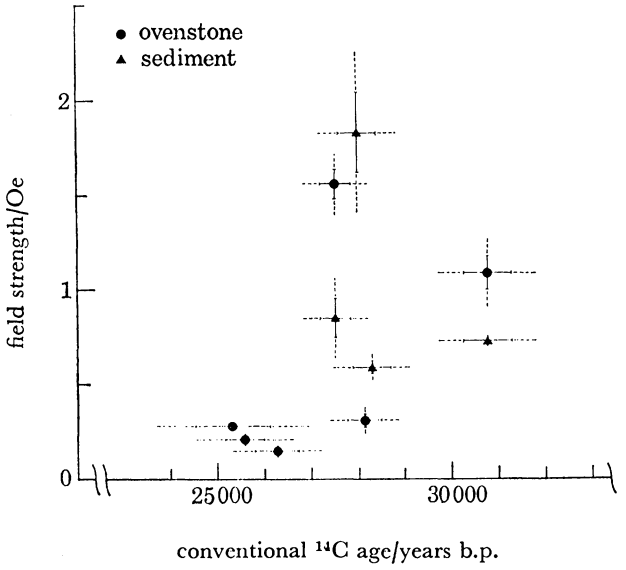

FIGURE 11. Mean ancient field strength measurements. Solid (dashed) lines show the experimental errors at the one (two) standard error level. Present day field at the locality is 0.6 Oe. Ovenstone and baked sediment means (table 3) for F7 and F9 are shown separately. These and the baked sediment means for F8 and F12 (the points above 0.5 Oe) are considered to be systematically *low* estimates of the ancient field strength, because of non-ideal behaviour during Thellier measurements. Data for F14 and S7, for which there are no radiocarbon ages, are not shown.

7. INTERPRETATION OF RESULTS

7.1. *Ancient field strengths*

The arguments outlined in §6 suggest that the true values of ancient field strength are close to the measured values when ideal behaviour occurred in the Thellier technique, and are higher than our measured values where non-ideal behaviour occurred. The data of table 3 are summarized in figure 11 to show the time variation of ancient field strength between 25000 and 31000 years ago. Bearing in mind that the present field strength at Lake Mungo is about 0.6 Oe then figure 11 shows that a very large increase in field strength occurred around 28000 years ago and there was low field strength around 26000 years ago. Each of these is associated with wide departures from the axial dipole field direction (table 2).

Fireplaces recording roughly the axial dipole field (F16, F17, F20) give field strengths of between 0.2 and 0.3 Oe. It is likely that F16 post-dates those fireplaces giving high ancient field strengths, but predates those with low values (F6 in particular). F17 and F20 appear to be younger than all the other fireplaces. Two other fireplaces, F14 and S7, also give wide departures associated with low field strengths. Because F16 records the present axial dipole field direction,

the simplest interpretation is that there were two different excursions of the geomagnetic field. The older excursion is associated with unusually high ancient field strengths around 30 000 to 28 000 years ago, while the younger excursion is associated with low field strengths around 26 000 years ago. Although no age information is available for F14 and S7, the low field strengths suggest they should be assigned to the younger excursion.

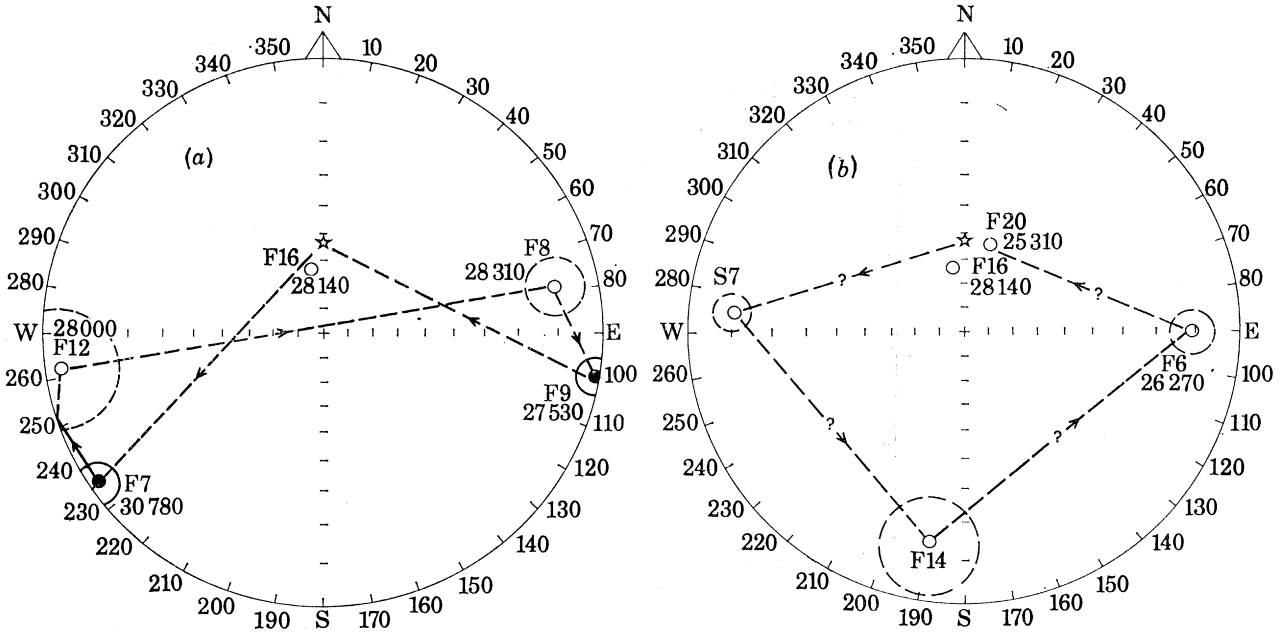

FIGURE 12. Stereographic projection of directions of magnetization observed during the two postulated geomagnetic excursions. Open (solid) circles are directions on the upper (lower) hemisphere. 95% circles of confidence are given for the means that depart widely from the axial dipole field direction (0°, −53°; shown by the star). Radiocarbon ages are given where available. (*a*) The Lake Mungo geomagnetic excursion characterized by abnormally high field strengths between 31 000 and 28 000 years B.P. (*b*) The postulated second geomagnetic excursion at about 26 000 years B.P. characterized by low field strengths.

7.2. *Directional changes*

Our interpretation of the combined directional and ancient field strength data is illustrated in figure 12 in the form of two geomagnetic excursions. The directional changes for the older high field strength excursion are essentially those reported earlier by Barbetti & McElhinny (1972). This is the *Lake Mungo Geomagnetic Excursion* (figure 12*a*). The field direction departs from the present field direction by up to 120° and the ancient field strength increases by a factor of five or six over what appears to be the background field strength outside the excursion. The increase in field strength is a factor of three over the present field strength. The duration of the excursion is at least as long as the difference in age between F7 (30 780 ± 520 years) and F16 (28 140 ± 370 years), that is 2640 ± 640 years. Taking into account the errors attached to the ages and the fact that the excursion is already underway at the time of F7, the likely range is between 2500 and 3000 years for the duration.

The younger low field strength excursion has not been reported before and we stress that our interpretation (figure 12*b*) is still tentative at this stage because of lack of age control on all fireplaces except F6. There is a clear case that F6 represents a distinct feature not related to the older fireplaces. It is clearly younger than F16 which records the normal field direction *after* the

high field strength excursion. Furthermore it is unique among the dated fireplaces recording wide departure from the present field direction in that it records the lowest field strength of this study at 0.15 Oe. The ancient field strength measurements show excellent agreement between ovenstones and baked sediment. It is not possible to estimate any time duration of the younger excursion because of lack of age control.

7.3. *Comparison with other excursions*

Geomagnetic excursions with dates younger than 40 000 years have now been recorded from many parts of the world. The occurrences have been summarized in table 6. Almost all of these have been recorded in lake or deep-sea sediments and it is extremely difficult to assess the reliability of ages assigned to them. The horizons are usually dated by assuming uniform sedimentation between or beyond ^{14}C dated horizons. Exceptions to this include the present study in which the ^{14}C dates refer directly to the archaeomagnetic data. Also, varve counting techniques as used in dating the excursions recorded in Sweden (Nöel & Tarling 1975) are generally regarded as being more reliable than ^{14}C dating. The only lavas recording a young excursion in the Puy de Laschamp have not been amenable to Potassium-Argon dating. A maximum age of 20 000 years was all that could be determined (Bonhommet & Zähringer 1969). The problem of interpreting the data of table 6 therefore revolves largely upon the extent to which the different ages may be taken as being significantly different from one another.

TABLE 6. SUMMARY OF LOCALITIES AND AGES FOR GEOMAGNETIC EXCURSIONS RECORDED OVER THE PAST 40 000 YEARS

locality	age/years	reference
Laschamp, France	8730–20 000	Bonhommet & Babkine (1967) Bonhommet & Zähringer (1969)
Gothenburg, Sweden (58° N, 12° E)	12 350–13 750	Mörner *et al.* (1971)
N. Atlantic Core A179-15 (25° N, 76° W)	12 250–~ 14 500	Mörner & Lanser (1975)
Lake Windermere, U.K. (54° N, 3° W)	13 400 ± 400	Mackereth (1971)
Swedish varves	12 400	Ising (1943)
Blekinge, Sweden (56° N, 15° E)	12 077–12 103 ± 150	Nöel & Tarling (1975)
Lake Erie, U.S.A. (42° N, 82° W)	⩾ 12 500	Creer (1974)
Tlapacoya, Mexico (19° N, 99° W)	14 450	Liddicoat *et al.* (1974)
Gulf of Mexico (24° N, 90° W)	12 500–17 000	Clark & Kennett (1973)
Gulf of Mexico (22° N, 94° W)	17 000 ± 1500	Freed & Healy (1974)
Lake Biwa, Japan (35° N, 136° E)	17 600–18 700	Nakajima *et al.* (1973)
Mono Lake, U.S.A. (38° N, 119° W)	24 000–24 600	Denham & Cox (1971)
Mono Lake, U.S.A. (38° N, 119° W)	24 600–25 000	Liddicoat & Coe (1975)
Lake Mungo, Australia (34° S, 143° E)	~ 26 000?	this paper
Lake Mungo, Australia (34° S, 143° E)	28 140–30 780	this paper
Gulf of Mexico (22° N, 94° W)	32 500 ± 1500	Freed & Healy (1974)
S. Indian Ocean Core RC8-39 (43° S, 42° E)	~ 40 000	Opdyke *et al.* (1974)

The ages listed in table 6 fall into two main groups, a younger one with ages spreading from 12 000 up to 19 000 years and an older one with ages from 24 000 to 32 000 years. Possible errors in the age determinations make it unlikely that all of these refer to the same excursion. But can it be supposed that each of these two groups represents a spread of ages from indeterminate dating of two excursions, the Laschamp and Lake Mungo excursions as supposed by Nöel & Tarling (1975)? One significant feature of the results listed is that the youngest ages

around 12000 to 14000 years are restricted to western Europe and possibly the eastern part of North America. The older ages up to 19000 years are from the Gulf of Mexico and Japan. Ages older than 24000 years occur in the southern Indian Ocean, Australia, the Gulf of Mexico and western North America. Interpretation of these results essentially depends upon the origin one places on these geomagnetic excursions. Possibilities include the following

(1) a tilt of the main dipole axis away from the axis of rotation,

(2) An aborted polarity change or enhanced non-dipole field during a period of diminished geomagnetic intensity,

(3) the occurrence of a very large intensity non-dipole feature over part of the Earth's surface.

The possibilities (1) and (2) would result in simultaneous world-wide effects, whereas (3) would not. Possibility (1) produces virtual geomagnetic poles recorded through the excursion that would be the same for every observer, but (2) and (3) would not. Although the distribution of ages could be the result of presently inadequate sampling of a world-wide event and imprecise dating, the grouping of ages over different parts of the Earth's surface suggests (3) as a likely mechanism. We therefore propose the following simple model for geomagnetic excursions.

It has been proposed that the isoporic foci formed by the intensity contours of the non-dipole field can be modelled as a set of radial dipoles situated in the outer part of the liquid-core (Lowes 1955). Bullard, Freedman, Gellman & Nixon (1950) suggested that the interaction of fluid eddies situated near the core-mantle boundary with the toroidal field might provide an origin for the non-dipole field. Suppose that one such eddy produces temporarily a greatly enhanced dipole moment, the region of the Earth's surface closest to this dipole would observe a greatly enhanced non-dipole field but points directly opposite in the other hemisphere would observe little or no effect. A dipole of strength $\frac{1}{8}$ of the main geocentric dipole and situated near the core-mantle boundary would produce a field of the same size as the main dipole at the nearest point on the Earth's surface. This could result in large local changes in field direction, coupled with either increase or decrease in field strength (depending on the dipole orientation) as the dipole grew and then decayed. At points on the Earth's surface furthest from the dipole the field produced would be only $\frac{1}{27}$ of the main field and almost no field changes would be observed.

The above process could explain why great increases in field strength were observed during the Lake Mungo excursion. However, the recent work of Shaw (1975) shows that sudden large increases in field strength can occur at the centre of a polarity transition. So whether or not this represents a chance enhancement of a non-dipole source during a polarity transition remains a mystery. Clearly more detailed ancient field strength measurements are needed during polarity transitions.

The time span of geomagnetic excursions is relatively short. Freed & Healy (1974) estimated 2500 years for their older excursion at 32500 years, as did Opdyke *et al.* (1974) for theirs at about 40000 years. Both these estimates agree very well with the estimate for the duration of the Lake Mungo excursion. Mörner & Lanser (1975) estimate 1400 years for the Gothenburg excursion, similar to 1100 years measured at Lake Biwa (Nakajima *et al.* 1973). The younger excursion of Freed & Healy (1974) at 17000 years is only estimated to be 600 ± 200 years duration, similar to the Denham & Cox (1971) estimate for the Mono Lake excursion ending at 24000 years. However, if the data of Liddicoat & Coe (1975) from Mono Lake are combined with those of Denham & Cox (1971), the large deviations in field direction extend over about 1000 years. All these estimates are very close to those for the time duration of polarity transitions (Ninkovich *et al.*

1966; Cox & Dalrymple 1967; McElhinny 1971). This might be regarded as some evidence in favour of the view that excursions are merely aborted reversals. However until their world-wide synchroneity is properly established, their origin must remain speculative.

References

Aitken, M. J. 1970 Dating by archaeomagnetic and thermoluminescent methods. *Phil. Trans. R. Soc. Lond.* A**269**, 77–88.

Allen, H. 1972 Where the crow flies backwards: Man and land in the Darling Basin. Ph.D. thesis, Australian National University, Canberra.

Barbetti, M. 1972 Geomagnetic field behaviour between 25000 yr and 35000 yr B.P. and its effect on atmospheric radiocarbon concentration: a current report. *Proc. 8th Intl Radiocarbon Dating Conference*, Wellington, New Zealand, 1972, pp. A104–13.

Barbetti, M. F. 1973*a* Archaeomagnetic and radiocarbon studies of aboriginal fireplaces. Ph.D. thesis, Australian National University, Canberra.

Barbetti, M. F. 1973*b* A furnace for archaeomagnetic and palaeomagnetic experiments. R.S.E.S. Publ. No. 997, Australian National University, Canberra.

Barbetti, M. & Allen, H. 1972 Prehistoric man at Lake Mungo, Australia, by 32000 yr B.P. *Nature, Lond.* **240**, 46–48.

Barbetti, M. & McElhinny, M. 1972 Evidence for a geomagnetic excursion 30000 yr. B.P. *Nature, Lond.* **239**, 327–330.

Barbetti, M. & Polach, H. 1973 A.N.U. Radiocarbon Data List V. *Radiocarbon* **15**, 241–251.

Bonhommet, N. & Babkine, J. 1967 Sur la présence d'aimantations inversées dans la Chaîne des Puys. *C.r. Hebd. Séanc. Acad. Sci., Paris*, B**264**, 92–94.

Bonhommet, N. & Zähringer, J. 1969 Paleomagnetism and potassium–argon age determinations of the Laschamp geomagnetic polarity event. *Earth Planet. Sci. Lett.* **6**, 43–46.

Bowler, J. M. 1971*a* Late Quaternary environments: a study of lakes and associated sediments in southeastern Australia. Ph.D. thesis, Australian National University, Canberra.

Bowler, J. M. 1971*b* Pleistocene salinities and climatic change: evidence from lakes and lunettes in southeastern Australia. In *Aboriginal Man and environment in Australia* (ed. D. J. Mulvaney and J. Golson, pp. 47–65). Canberra: Australian National University Press.

Bowler, J. M., Jones, R., Allen, H. & Thorne, A. G. 1970 Pleistocene human remains from Australia: a living site and human cremation from Lake Mungo, western New South Wales. *World Archaeology* **2**, 39–60.

Bullard, E. C., Freedman, C., Gellman, H. & Nixon, J. 1950 The westward drift of the Earth's magnetic field. *Phil. Trans. R. Soc. Lond.* A**243**, 67–92.

Clark, H. C. & Kennett, J. P. 1973 Paleomagnetic excursion recorded in latest Pleistocene deep-sea sediments, Gulf of Mexico. *Earth Planet. Sci. Lett.* **19**, 267–274.

Coe, R. S. 1967*a* Paleointensities of the Earth's magnetic field determined from Tertiary and Quaternary rocks. *J. geophys. Res.* **72**, 3247–3262.

Coe, R. S. 1967*b* The determination of paleointensities of the Earth's magnetic field with emphasis on mechanisms which could cause non-ideal behaviour in Thellier's method. *J. Geomag. Geoelect.* **19**, 157–179.

Collinson, D. W. 1968 An estimate of the haematite content of sediments by magnetic analysis. *Earth Planet. Sci. Lett.* **4**, 417–421.

Cox, A. 1969 Geomagnetic reversals. *Science, N.Y.* **163**, 237–245.

Cox, A. & Dalrymple, G. B. 1967 Statistical analysis of geomagnetic reversal data and the precision of potassium–argon dating. *J. geophys. Res.* **72**, 2603–2614.

Creer, K. M. 1974 Unsteady geomagnetic reversals in the Late Pleistocene. *Eos. Trans. Am. Geophys. Un.* **55**, 224.

Dagley, P. & Lawley, E. 1974 Palaeomagnetic evidence for the transitional behaviour of the geomagnetic field. *Geophys. J. R. astron. Soc.* **36**, 577–598.

Denham, C. R. & Cox, A. 1971 Evidence that the Laschamp polarity event did not occur 13300–30400 years ago. *Earth Planet. Sci. Lett.* **13**, 181–190.

Doell, R. R. 1972 Palaeomagnetic studies of Icelandic lava flow. *Geophys. J. R. astron. Soc.* **26**, 459–479.

Doell, R. R. & Cox, A. 1972 The Pacific geomagnetic secular variation anomaly and the question of lateral uniformity in the lower mantle. In *The nature of the solid Earth* (ed. E. C. Robertson, J. F. Hays and L. Knopoff), pp. 245–284. New York: McGraw-Hill.

Doell, R. R. & Dalrymple, G. B. 1973 Potassium–argon ages and paleomagnetism of the Waianae and Koolau Volcanic Series, Oahu, Hawaii. *Geol. Soc. Am. Bull.* **84**, 1217–1242.

Ellwood, B. B., Watkins, N. D., Amerigian, C. & Self, S. 1973 Brunhes epoch geomagnetic secular variation on Terceira Island, Central North Atlantic. *J. geophys. Res.* **78**, 8699–8710.

Fisher, R. A. 1953 Dispersion on a sphere. *Proc. R. Soc. Lond.* A **217**, 295–305.

PHILOSOPHICAL TRANSACTIONS OF THE ROYAL SOCIETY A MATHEMATICAL, PHYSICAL & ENGINEERING SCIENCES

Freed, W. K. & Healy, N. 1974 Excursions of the Pleistocene geomagnetic field recorded in Gulf of Mexico sediments. *Earth Planet. Sci. Lett.* **24**, 99–104.

Hedley, I. G. 1968 Chemical remanent magnetization of the $FeOOH.Fe_2O_3$ system. *Phys. Earth Planet. Interiors* **1**, 103–121.

Ising, G. 1943 On the magnetic properties of varved clay. *Ark. Mat. Astr. Phys.* **29**A, 1–37.

Kobayashi, K. 1959 Chemical remanent magnetization of ferromagnetic minerals and its application to rock magnetism. *J. Geomag. Geoelect.* **10**, 99–117.

Lawley, E. 1970 The intensity of the geomagnetic field in Iceland during Neogene polarity transitions and systematic deviations. *Earth Planet. Sci. Lett.* **10**, 145–149.

Levi, S. 1974 Some magnetic properties of magnetite as a function of grain size and their implications for paleomagnetism. Ph.D. thesis, University of Washington, Seattle.

Liddicoat, J. C. & Coe, R. S. 1975 Mono Lake 24,000 year B.P. geomagnetic excursion: Additional data. *Eos. Trans. Am. Geophys. Un.* **56**, 978.

Liddicoat, J. C., Coe, R. S., Lambert, P. W. & Valastro, S. Jr. 1974 Dating Mexican archaeological sites using a possible Late Quarternary geomagnetic field excursion. *Geol. Soc. Am. Abstracts with programs* (1974 Annual Meeting, Miami) **6**, 845.

Lowes, F. J. 1955 Secular variation and the non-dipole field. *Ann. Geophys.* **11**, 91–94.

Mackereth, F. J. H. 1971 On the variation in direction of the horizontal component of remanent magnetization in lake sediments. *Earth Planet Sci. Lett.* **12**, 332–338.

Manwaring, E. A. 1971 Astatic magnetometer designed and built by the Bureau of Mineral Resources. *Bur. Min. Resour.* (*Australia*), Record No. 1971/54, 54 pp.

McElhinny, M. W. 1971 Geomagnetic polarity transitions. *Comments on Earth Sci.*: *Geophys.* **1**, 150–158.

McElhinny, M. W., Luck, G. R. & Edwards, D. 1971 A large volume magnetic field free space for thermal demagnetization and other experiments in palaeomagnetism. *Pure appl. Geophys.* **90**, 126–130.

Mörner, N. A. & Lanser, J. 1975 Paleomagnetism in deep-sea core A179-15. *Earth Planet. Sci. Lett.* **26**, 121–124.

Mörner, N. A., Lanser, J. P. & Hospers, J. 1971 Late Weichselian palaeomagnetic reversal. *Nature, Phys. Sci.* **234**, 173–174.

Nagata, T., Arai, Y. & Momose, K. 1963 Secular variation of the total geomagnetic force during the last 5000 years. *J. geophys. Res.* **68**, 5277–5281.

Nakajima, T., Yaskawa, K., Natsuhara, N., Kawai, N. & Horie, S. 1973 Very short-period geomagnetic excursion 18000 yr B.P. *Nature, Phys. Sci.* **244**, 8–10.

Ninkovich, D., Opdyke, N. D., Heezen, B. C. & Foster, J. H. 1966 Paleomagnetic stratigraphy, rates of deposition and tephrachronology in North Pacific deep-sea sediments. *Earth Planet. Sci. Lett.* **1**, 476–492.

Nöel, M. & Tarling, D. H. 1975 The Laschamp geomagnetic 'event'. *Nature, Lond.* **253**, 705–707.

Opdyke, N. D., Shackleton, N. J. & Hays, J. D. 1974 The details of a magnetic excursion as seen in a piston core from the Southern Indian ocean. *Eos. Trans. Am. Geophys. Un.* **55**, 237.

Porath, H. 1968 Magnetic studies on specimens of intergrown maghemite and hematite. *J. geophys. Res.* **73**, 5959–5965.

Schwarz, E. J. & Christie, K. W. 1967 Original remanent magnetization of Ontario potsherds. *J. geophys. Res.* **72**, 3263–3269.

Shaw, J. H. 1975 Strong geomagnetic fields during a single Icelandic polarity transition. *Geophys. J. R. Astron. Soc.* **40**, 345–350.

Smith, P. J. 1967 The intensity of the ancient geomagnetic field: A review and analysis. *Geophys. J. R. Astron. Soc.* **12**, 321–362.

Strangway, D. W., Honea, R. M., McMahon, B. E. & Larson, E. E. 1968 The magnetic properties of naturally occurring goethite. *Geophys. J. R. Astron. Soc.* **15**, 345–349.

Strangway, D. W., McMahon, B. E. & Bischoff, J. L. 1969 Magnetic properties of minerals from the Red Sea thermal brines. In *Hot brines and recent heavy metal deposits in the Red Sea – A geochemical and geophysical account* (ed. E. T. Degens and D. A. Ross), pp. 460–473. New York: Springer Verlag.

Thellier, E. 1951 Proprietés magnétiques des terres cuites et des roches. Rapport au colloque sur le ferromagnétisme et l'antiferromagnétism, Grenoble 1950. *J. de Phys.* **12**, 205–218.

Thellier, E. & Thellier, O. 1959 Sur l'intensité du champ magnétique terrestre dans le passé historique et géologique. *Ann. Geophys.* **15**, 285–376.

Vlasov, A. Ya & Gornushkina, N. A. 1973 Chemical remanent magnetization during the lepidocrocite–maghemite–hematite temperature transformation. *Izv. Acad. Sci. U.S.S.R. Physics of the Solid Earth*, **2**, 110–115.

Watkins, N. D. 1973 Brunhes epoch geomagnetic secular variation on Reunion Island. *J. geophys. Res.* **78**, 7763–7768.

Watkins, N. D. & Nougier, J. 1973 Excursions and secular variation of the Brunhes epoch geomagnetic field in the Indian Ocean region. *J. geophys. Res.* **78**, 6060–6068.

Wilson, R. L., Dagley, P. & McCormack, A. G. 1972 Palaeomagnetic evidence about the source of the geomagnetic field. *Geophys. J. R. Astron. Soc.* **28**, 213–224.

PHILOSOPHICAL TRANSACTIONS OF THE ROYAL SOCIETY A MATHEMATICAL, PHYSICAL & ENGINEERING SCIENCES